

Tunable Eigenvector-Based Centralities for Multiplex and Temporal Networks *

Dane Taylor[†], Mason A. Porter[‡], and Peter J. Mucha[§]

Abstract.

Characterizing the importances (i.e., centralities) of nodes in social, biological, information, and technological networks is a core topic in both network science and data science. We present a linear-algebraic framework that generalizes eigenvector-based centralities, including PageRank and hub/authority scores, to provide a common framework for two popular classes of multilayer networks: multiplex networks (which have layers that encode different types of relationships) and temporal networks (in which the relationships change over time). Our approach involves the study of joint, marginal, and conditional “supracentralities” that one can calculate from the dominant eigenvector of a *supracentrality matrix* [Taylor et al., 2017], which couples centrality matrices that are associated with the individual network layers. We extend this prior work (which was restricted to temporal networks with layers that are coupled by undirected, adjacent-in-time coupling) by allowing the layers to be coupled through a (possibly asymmetric) interlayer-adjacency matrix \mathbf{A} , in which entry $A_{tt'} > 0$ gives the coupling between layers t and t' . Our framework provides a unifying foundation for centrality analysis of multiplex and temporal networks; and it reveals a complicated dependency of the supracentralities on the topology and weights of interlayer coupling. By scaling \mathbf{A} by an interlayer coupling strength $\omega \geq 0$ and developing a singular perturbation theory for the limits of weak ($\omega \rightarrow 0^+$) and strong coupling ($\omega \rightarrow \infty$), we also reveal an interesting dependence of supracentralities on the dominant left and right eigenvectors of \mathbf{A} . We provide additional theoretical and practical insights by applying our framework to two empirical data sets: a multiplex-network representation of airline transportation in Europe and a temporal network that encodes the graduation and hiring of mathematicians at U.S. colleges and universities.

Key words. Network science, Multilayer networks, Data integration, Ranking systems, Perturbation theory

AMS subject classifications. 91D30, 05C81, 94C15, 05C82, 15A18

1. Introduction. Quantifying the importance of entities in a network representation of a data set is an essential feature of many internet search engines [11, 33, 60, 78], ranking algorithms for sports teams and athletes [12, 15, 93], targeted social-network marketing schemes [52], investigations of fragility in infrastructures [40, 43], quantitative analysis of the impact of research papers and scientists [31], research on the influence of judicial and legislative documents [32, 61], identification of novel drug targets in biological systems [49], and many other applications. In the most common (and simplest) type of network, called a “graph” or a “monolayer network”, a node represents an entity (e.g., web pages, persons, documents, proteins, etc.), and an edge encodes a relationship between a pair of entities. *Centrality analysis*, in which one seeks to quantify the importances of nodes and/or edges (and, more generally, of

*We thank Deryl DeFord, Tina Eliassi-Rad, Des Higham, Christine Klymko, Marianne McKenzie, Scott Pauls, and Michael Schaub for fruitful conversations. DT was supported by the Simons Foundation under Award #578333. PJM was supported by the Eunice Kennedy Shriver National Institute of Child Health & Human Development of the National Institutes of Health under Award Number R01HD075712 and by the James S. McDonnell Foundation 21st Century Science Initiative - Complex Systems Scholar Award grant #220020315. The content is solely the responsibility of the authors and does not necessarily reflect the views of any of the funding agencies.

[†]Department of Mathematics, University at Buffalo, State University of New York, Buffalo, NY 14260, USA

[‡]Department of Mathematics, University of California, Los Angeles, CA 90095, USA

[§]Carolina Center for Interdisciplinary Applied Mathematics, Department of Mathematics and Department of Applied Physical Sciences, University of North Carolina, Chapel Hill, NC 27599, USA

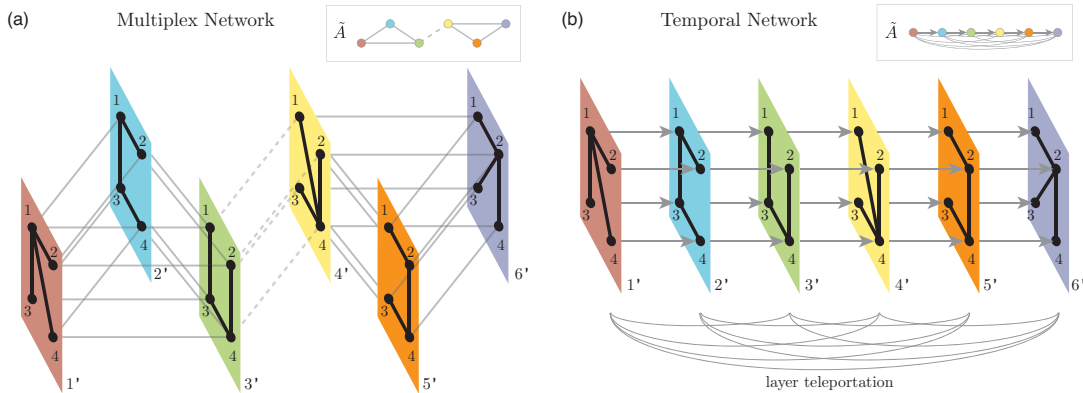


Figure 1. Schematics of two types of multilayer networks. (a) A multiplex network, in which layers are coupled categorically. (b) A multiplex representation of a discrete-time temporal network, where we couple the sequence of layers through a directed (time-respecting) chain with “layer” teleportation. (See Sec. 5.2 for a definition.) Each inset depicts the interlayer-coupling topology, which we encode (along with interlayer edge weights) in an interlayer-adjacency matrix $\bar{\mathbf{A}}$. We assume that the interlayer couplings are “diagonal” and “uniform” (see Sec. 2.2), and we take their weights to be $\omega \geq 0$. As we illustrate in panels (a) and (b), the interlayer coupling can be either undirected or directed.

other subgraphs as well), has been developed intensively across numerous domains, including sociology, mathematics, computer science, and physics [19, 33, 60, 75].

Meanwhile, scholars have developed increasingly comprehensive network representations to help with data integration [54, 77], including the generalization of graphs to *multilayer networks* [8, 18, 54, 82] and of centrality measures for multilayer and temporal networks [2, 27, 38, 39, 42, 53, 62, 71, 80, 90, 92, 94, 95, 99, 100, 105, 114, 115]. Multilayer network centralities have been used in the study of diverse applications, including social networks [14, 17, 42, 65, 66], transportation systems [22, 48, 101, 110], economic systems [5, 24, 25], neural systems [6, 20, 48, 116], and signal processing of geological time series [64]. Moreover, many techniques in centrality analysis are closely connected to the study of various dynamical processes (including in multilayer networks), such as random walks [26, 33, 35, 42, 70, 76], information spreading [17, 88], and congestion [22].

We consider two types of multilayer networks (see Fig. 1): (1) *multiplex networks*, in which layers represent different types of relationships; and (2) *temporal networks*, in which layers represent different points or periods in time. We further develop the mathematical framework of *supracentrality* matrices, which we developed recently [105] to generalize eigenvector-based centralities — e.g., PageRank [11, 33, 78], eigenvector centrality [10], and hub and authority scores [56] — to multilayer representations of discrete-time temporal networks. Our approach involves coupling centrality matrices associated with the individual layers into a larger supracentrality matrix and studying the latter’s dominant eigenvector to obtain *joint*, *marginal*, and *conditional* centralities (see Sec. 3.2) to quantify the importances of nodes, layers, or node-layer pairs. In this article, we extend the supracentrality framework of [105] to multiplex networks, which integrate multiple data sets by coupling them as layers in a single multilayer network.

Generalizing centrality measures to multiplex networks and temporal networks are active

areas of research [8, 18, 44, 45, 54] (see our discussion in Sec. 2.3), and the supracentrality framework that we discuss is relevant for such efforts.¹ Our original formulation of supracentrality in [105] focused on temporal networks, and it assumed a specific type of multilayer representation with adjacent-in-time coupling. We now extend supracentrality matrices to a broader class of multilayer networks by coupling layers via an interlayer-adjacency matrix $\tilde{\mathbf{A}}$, where $\tilde{A}_{tt'} \geq 0$ encodes the (possibly asymmetric) coupling between layers t and t' . We assume “diagonal” interlayer coupling (see Sec. 2.2 and [54]), as we only connect instantiations of the same entity (i.e., node) across different layers. We also assume that the interlayer coupling is “uniform”, so all edges between layers t and t' have the same edge weight $\omega \tilde{A}_{tt'} \geq 0$. Multilayer networks with both diagonal and uniform interlayer coupling are said to be “layer-coupled” [54]. The value of ω determines how strongly the layers influence each other. We will show that choices for $\tilde{\mathbf{A}}$ and ω significantly affect supracentralities and are useful “tuning knobs” to consider in calculating and interpreting supracentralities.

To gain theoretical insight into the effects of $\tilde{\mathbf{A}}$ and ω , we develop a singular perturbation theory to analyze the dominant eigenspace of supracentrality matrices in the limits of weak ($\omega \rightarrow 0^+$) and strong ($\omega \rightarrow \infty$) coupling. We show that these limits implement, respectively, layer decoupling and a type of layer aggregation (which is a form of data fusion). There are many scenarios in which one couples matrices into a larger “supramatrix” — e.g., the detection of multilayer community structure using a supramodularity matrix [72, 113] and the study of random walks and diffusion on multilayer networks via supra-Laplacian matrices [35, 86] — and our perturbative approach reveals insights about the utility of matrix coupling as a general technique for multimodal data integration. Specifically, our singular perturbation theory of Sec. 4 makes no explicit assumption that the block-diagonal matrices are centrality matrices, so our results also characterize the dominant eigenspaces for layer-coupled matrices in other applications, including ones that are unrelated to networks.

Our results in Sec. 4 characterize the decoupling and aggregation limits of supracentrality matrices. We illustrate that the limiting dominant eigenspace of a supracentrality matrix depends on a complicated interplay between many factors, including (i) the dominant eigenvectors for the centrality matrix of each layer; (ii) the dominant eigenvectors for the interlayer-adjacency matrix; and (iii) the spectral radii of the layers’ centrality matrices. For the $\omega \rightarrow \infty$ limit, the dominant eigenspace of a supracentrality matrix depends on a weighted average of the layers’ centrality matrices, with weights that are related to the dominant eigenspace of $\tilde{\mathbf{A}}$. A key factor for the $\omega \rightarrow 0^+$ limit is whether the layers’ individual centrality matrices have identical or different spectral radii. In the latter scenario, we identify and characterize an eigenvector-localization phenomenon, in which one or more layers dominate the decoupling limit. Our layer-aggregation and decoupling limits are reminiscent of prior research on supra-Laplacian matrices [35, 97], but our coupling matrices and qualitative results both differ from such prior work.

We illustrate our framework with applications to two empirical, multimodal network data sets. First, we study the importances of European airports in a multiplex network in which layers represent different airlines [13]. We find, for example, that supracentralities in the

¹In principle, one can also use supracentrality matrices of higher dimensionality to study networks that are both multiplex and temporal, but we do not study such an example in this paper.

weak-coupling limit are dominated by the Ryanair layer, which among all layers has the most edges and an adjacency matrix with the largest spectral radius. For intermediate coupling strengths, we observe a centrality “boost” (i.e., an increase relative to the centralities of other nodes) for airports that are central *both* to the Ryanair layer and to a network that is associated with an aggregation of the network layers (specifically, the one from summing the layers’ adjacency matrices). We study these phenomena by comparing marginal node centralities to the nodes’ intralayer degrees and total degrees (which quantify, respectively, the number of edges in each layer and the total number of edges across all layers). Our second focal data set is based on the Mathematics Genealogy Project [85, 103] and is a temporal network that encodes the graduation and hiring of mathematicians at mathematical-science Ph.D. programs in the United States [105]. Extending [105], we now explore the effects of causality by implementing time-directed interlayer coupling along with *layer teleportation* (see Fig. 1(b) and our discussion in Sec. 5.2), which we define analogously to *node teleportation* in PageRank [33]. Similar to previous findings for causality-respecting centralities [29, 37], our approach boosts the centralities of node-layer pairs whose edges occur earlier in time (allowing them to causally influence more nodes). Specifically, this phenomenon manifests as a boost in marginal layer centrality for older time layers. Our numerical experiments highlight the importance of exploring a diverse set of interlayer-coupling architectures $\tilde{\mathbf{A}}$ and strengths ω to identify application-appropriate parameter choices.

Our paper is organized as follows. In Sec. 2, we present background information on eigenvector-based centralities, multiplex and temporal networks, and generalizing centralities for such networks. In Sec. 3, we present our supracentrality framework. In Sec. 4, we analyze the weak-coupling and strong-coupling limits. In Sec. 5, we study the two empirical data sets. We conclude in Sec. 6 and give the proofs for our main mathematical results in appendices. We present further numerical investigations in Supplementary Material.

2. Background Information. We present background information on eigenvector-based centralities in Sec. 2.1, multiplex and temporal networks in Sec. 2.2, and extensions of centrality for multiplex and temporal networks in Sec. 2.3.

2.1. Eigenvector-Based Centrality Measures. We start with a definition.

Definition 2.1 (Monolayer Network). *Let $\mathcal{G}(\mathcal{V}, \mathcal{E})$ be a monolayer (i.e., single-layer) network with nodes $\mathcal{V} = \{1, 2, \dots, N\}$ and a set $\mathcal{E} \subset \mathcal{V} \times \mathcal{V} \times \mathbb{R}_+$ of positively-weighted edges, where $(i, j, w_{ij}) \in \mathcal{E}$ if and only if there exists an edge from i to j with weight w_{ij} . We also encode this network (which is a weighted graph) by an $N \times N$ adjacency matrix \mathbf{A} with entries $A_{ij} = w_{ij}$ if $(i, j, w_{ij}) \in \mathcal{E}$ and $A_{ij} = 0$ otherwise.*

One of the most popular approaches for quantifying the importances of nodes \mathcal{V} in a network is to calculate the dominant eigenvector of a network-related matrix and interpret the eigenvector’s entries as a proxy for importance [33, 75].²

Definition 2.2 (Eigenvector-Based Centrality). *Let $\mathbf{C} = C(\mathbf{A})$ be a “centrality matrix” obtained via some function $C : \mathbb{R}^{N \times N} \mapsto \mathbb{R}^{N \times N}$ of the adjacency matrix \mathbf{A} for a network*

²There are also other centralities, such as Katz centrality, that involve eigenvectors but are not equal to the entry of a dominant eigenvector [75].

$\mathcal{G}(\mathcal{V}, \mathcal{E})$. Consider the right dominant eigenvector \mathbf{u} , the solution of

$$(2.1) \quad \mathbf{C}\mathbf{u} = \lambda_{\max}\mathbf{u},$$

where $\lambda_{\max} \in \mathbb{R}$ is the largest eigenvalue of \mathbf{C} . Each entry u_i specifies the eigenvector-based centrality associated with the function C for node $i \in \mathcal{V}$.

Different choices for $C(\mathbf{A})$ yield different notions of centrality, and some are more useful than others. The following are among the most popular eigenvector-based centralities.

Definition 2.3 (Eigenvector Centrality [10]). With the choice $\mathbf{C}^{(EC)} = \mathbf{A}$, Eq. (2.1) yields eigenvector centralities $\{u_i^{(EC)}\}$.

Definition 2.4 (Hub and Authority Scores [56]). With the choices $\mathbf{C}^{(HS)} = \mathbf{A}\mathbf{A}^T$ and $\mathbf{C}^{(AS)} = \mathbf{A}^T\mathbf{A}$, Eq. (2.1) yields hub scores $\{u_i^{(HS)}\}$ and authority scores $\{u_i^{(AS)}\}$, respectively.

Remark 2.1. Hub scores and authority scores are, respectively, the dominant left and right singular vectors of \mathbf{A} .

Definition 2.5 (PageRank [33,78]). Consider the choice $\mathbf{C}^{(PR)} = \sigma\mathbf{A}\mathbf{D}^{-1} + (1-\sigma)N^{-1}\mathbf{1}\mathbf{1}^T$, where \mathbf{D} is a diagonal matrix that encodes the node degrees (i.e., $D_{ij} = \delta_{ij} \sum_j A_{ij}^T$), the quantity $\sigma \in [0, 1]$ is a “node” teleportation parameter (we will assume that $\sigma = 0.85$ in this paper), and $\mathbf{1}$ is a length- N vector of ones (such that $\mathbf{1}\mathbf{1}^T$ is an $N \times N$ matrix of ones). Using this choice in Eq. (2.1), we obtain PageRank centralities $\{u_i^{(PR)}\}$.

Remark 2.2. It is also common to compute PageRank centralities from a left eigenvector [33]. In the present paper, we use a right-eigenvector formulation to be consistent with the other eigenvector-based centralities. One can recover the other formulation by taking the transpose of Eq. (2.1).

Remark 2.3. There are other possible teleportation strategies for PageRank, such as ones with local bias or emphasis on other features [33]. In such cases, one replaces the matrix $\mathbf{1}\mathbf{1}^T$ by $\mathbf{u}\mathbf{1}^T$, where the vector \mathbf{u} encodes the biases.

In most applications, it is important to choose the function C to ensure that centralities are unique and strictly positive. It is common to use the following two theorems to guarantee these important features.

Theorem 2.6 (Perron–Frobenius Theorem for Nonnegative Matrices [4]). Let $\mathbf{C} \in \mathbb{R}^{N \times N}$ be an irreducible square matrix with nonnegative entries. It then follows that \mathbf{C} has a simple largest positive eigenvalue λ_{\max} and that its left and right eigenvectors are positive and unique. Moreover, if \mathbf{C} is aperiodic (i.e., $\mathbf{C} \neq \mathbf{C}^k$ for any $k > 1$), then λ_{\max} is a dominant eigenvalue: $|\lambda_i| < \lambda_{\max}$ for $i \neq \operatorname{argmax}_{i \in \mathcal{V}} |\lambda_i|$.

Theorem 2.7 (Strong Connectivity Implies Irreducibility [4]). Consider the (possibly weighted and directed) network associated with a nonnegative square matrix \mathbf{C} . If the associated network is strongly connected (i.e., there exists a path from any origin node to any destination node), then \mathbf{C} is irreducible.

One typically seeks a centrality matrix \mathbf{C} that is irreducible (or equivalently, a matrix such that its associated network defined by the weighted edges $\{(i, j, C_{ij})\}$ is strongly connected).

Ensuring irreducibility is an important consideration when introducing new types of centrality (including ones with both positive and negative edges [28]). For example, the term $(1 - \alpha)N^{-1}\mathbf{1}\mathbf{1}^T$ in Definition 2.5 implies that $\mathbf{C}^{(PR)}$ is positive (i.e., $C_{ij}^{(PR)} > 0$ for every $i, j \in \mathcal{V}$), which ensures that $\mathbf{C}^{(PR)}$ is irreducible, regardless of whether the network with adjacency matrix \mathbf{A} is strongly connected [33].

Before continuing, we highlight an eigenvector-based centrality measure that uses both the left and right eigenvectors and therefore does not exactly fit Definition 2.2. Specifically, one defines the *dynamical importance* of a node in terms of the change of the leading eigenvalue of \mathbf{A} under removal of that node from the network [89] (see also [109]). In practice, as shown in [89], one can approximate dynamical importance to first order (provided one does not lose strong connectivity when removing the node) with an expression that depends on the leading right and left eigenvectors of \mathbf{A} . Other eigenvector-based centralities that involve two or more eigenvectors obtained through matrix perturbations have been developed to cater to particular applications, including disease spreading [104, 106], percolation [89, 107], and synchronization of dynamical systems [108]. Such analysis of perturbations of dynamical systems on networks is also related to notions of eigenvalue and eigenvector elasticities [36, 50, 51].

2.2. Multiplex and Temporal Networks. The different layers of a multilayer network can encode different types of connections and/or interacting systems [54], including interconnected critical infrastructures [41], categories of social ties [58], networks at different instances in time [112], and many others. By considering the various possibilities for interactions between nodes within and across layers, one can obtain a taxonomy for different types of multilayer networks [54]. We focus on two popular situations: *multiplex networks*, in which different layers represent different types of interactions; and *temporal networks*, in which layers represent different time instances or time periods. We provide formal definitions that are salient for these last two situations. It is convenient for both temporal and multiplex networks to refer to a given node i in a given layer t as a *node-layer pair* (i, t) .

Definition 2.8 (Uniformly and Diagonally-Coupled (i.e., Layer-Coupled) Multiplex Network). Let $\mathcal{G}(\mathcal{V}, \{\mathcal{E}^{(t)}\}, \tilde{\mathcal{E}})$ be a multilayer network with nodes $\mathcal{V} = \{1, \dots, N\}$ and T layers, with interactions between node-layer pairs encoded by the sets $\{\mathcal{E}^{(t)}\}$ of weighted edges, where $(i, j, w_{ij}^t) \in \mathcal{E}^{(t)}$ if and only if there is an edge (i, j) with weight w_{ij}^t in layer t . The set $\tilde{\mathcal{E}} = \{(s, t, \tilde{w}_{st})\}$ encodes the topology and weights for coupling separate instances of the same node between a pair of layers $(s, t) \in \{1, \dots, T\} \times \{1, \dots, T\}$. Equivalently, one can encode a multiplex network as a set $\{\mathbf{A}^{(t)}\}$ of adjacency matrices, such that $A_{ij}^{(t)} = w_{ij}^t$ if $(i, j, w_{ij}^t) \in \mathcal{E}^{(t)}$ and $A_{ij}^{(t)} = 0$ otherwise, along with an interlayer-adjacency matrix $\tilde{\mathbf{A}}$ with components $\tilde{A}_{st} = \tilde{w}_{st}$ if $(s, t, \tilde{w}_{st}) \in \tilde{\mathcal{E}}$ and $\tilde{A}_{ij}^{(t)} = 0$ otherwise.

See Fig. 1(a) for a pedagogical example of a small multiplex network. The multiplex coupling in Definition 2.8 is “diagonal” because we only allow coupling between a node in one layer and that same node in other layers, and it is “uniform” because the coupling between two layers is identical for all nodes in those two layers. A multilayer network with both of these conditions is called “layer-coupled” [54]. Our choice to represent interlayer couplings via $\tilde{\mathbf{A}}$ is a generalization of the special, but common, case in which the interlayer edge weights

are identical for all layer pairs (i.e., $\tilde{\omega}_{st} = \omega$ for any s and t). Although there are many other coupling strategies [9, 54], we focus on uniform and diagonal coupling because it is one of the simplest and most popular coupling schemes. Additionally, the interlayer-adjacency matrix $\tilde{\mathbf{A}}$ allows a great deal of flexibility and fine tuning. Moreover, as we will describe in Sec. 3, these restrictions impose matrix symmetries that we can exploit to derive results for when the layers are coupled either very weakly or very strongly.

We use a similar multilayer network representation to study temporal networks.

Definition 2.9 (Discrete-Time Temporal Network). *A discrete-time temporal network consists of nodes $\mathcal{V} = \{1, \dots, N\}$ and a sequence of network layers. We denote it either as $\mathcal{G}(\mathcal{V}, \{\mathcal{E}^{(t)}\})$ or by a sequence $\{\mathbf{A}^{(t)}\}$ of adjacency matrices such that $A_{ij}^{(t)} = w_{ij}^t$ if $(i, j, w_{ij}^t) \in \mathcal{E}^{(t)}$ and $A_{ij}^{(t)} = 0$ otherwise. A discrete-time temporal network can also include coupling between layers.*

Note that Definition 2.9 makes no explicit assumptions about how the layers are coupled. That is, a discrete-time temporal network consists of a set of nodes and an ordered set of layers. It is common, however, for investigations of temporal networks to introduce coupling between time layers, such as by representing them (as we do) as a multiplex network with a diagonal interlayer coupling that respects time.

2.3. Extensions of Centrality for Multiplex and Temporal Networks. There has been a recent explosion of research on centrality measures for multilayer networks [18, 54]. Much of this work is related to work on generalizing network properties such as node degree [7, 21, 66, 101] and shortest paths, with the latter leading to generalizations of notions such as betweenness centrality [14, 65, 95, 96] and closeness centrality [66, 96]. Of particular relevance to the present paper are generalizations of eigenvector-based centralities to multiplex networks. Salient notions that have been generalized include eigenvector centrality [7, 21, 24, 25, 94], hub and authority scores [57, 87, 98, 110], and PageRank [26, 42, 76]. These extensions have employed various strategies, several of which we discuss briefly.

One strategy is to represent a multiplex network as a tensor and use tensor decompositions [57]. Another strategy is to define a system of centrality dependencies in which high-centrality elements (nodes, layers, and so on) connect to other high-centrality elements, and one simultaneously solves for multiple types of centrality [87, 98, 110] as a fixed-point solution of the system of (possibly nonlinear) dependencies. For example, [87] and [110] defined centralities for both nodes and layers such that highly-ranked layers contain highly-ranked nodes and highly-ranked nodes are in highly-ranked layers. In a third strategy, which is the one that most closely resembles our present approach, one constructs a *supramatrix* of size $NT \times NT$ for N nodes and T layers, such that the centralities of node-layer pairs $\{(i, t)\}$ are given by the dominant eigenvector of the supramatrix. For example, [24, 25, 91, 94] constructed a supramatrix by using the Khatri–Rao matrix product between a matrix that encodes interlayer connections and a block matrix that has the layers’ adjacency matrices as columns. Another approach involves computing one or more centralities independently for each layer and using consensus ranking [83], and one can also generalize monolayer centrality measures to construct multilayer “versatility” measures [23].

There have also been many efforts to extend centralities to temporal networks. There

are extensive discussions of such efforts in [105] and [63]. To add to these lists, we briefly highlight contributions that appeared recently or were not mentioned in [105]. Arrigo and Higham [3] introduced a method to efficiently estimate temporal communicability (a generalization of Katz centrality), which has been applied to a variety of applications, including neuroscience [67] and disease spreading [16, 68]. Huang and Yu [46] extended a measure called dynamic-sensitive centrality to temporal networks. References [30, 47, 84] introduced variants of eigenvector centrality for temporal networks. We highlight [30] in particular, because it explored connections between continuous and discrete-time calculations of temporal centralities. Nathan et al. [73] introduced an efficient algorithm for computing exponential centrality for streaming graphs. Although methods for streaming and continuous-time networks are important (see, e.g., [1] for a generalization of PageRank to such situations), we restrict our attention to discrete-time temporal networks in an effort to further bridge the literatures on temporal and multiplex networks.

In Sec. 3, we introduce a new construction for a supracentrality matrix that is based on a Kronecker product. This construction generalizes our previous work [105], where we introduced a supracentrality framework for temporal networks and assumed adjacent-in-time coupling (i.e., $\tilde{A}_{tt'} = 1$ for $|t - t'| = 1$ and $\tilde{A}_{tt'} = 0$ otherwise). Our new formulation introduces an interlayer-adjacency matrix $\tilde{\mathbf{A}}$, allowing our framework to flexibly cater to either multiplex or temporal networks. It is also important to note that there are also multilayer representations of temporal networks that are not multiplex. One such approach is to connect each node-layer pair (i, t) to $\{(j, t + 1)\}$ for $j \in \{j : A_{ij}^{(t)} \neq 0\}$, yielding a supra-adjacency matrix with identity matrices on the block diagonal and the layers' adjacency matrices on the off-diagonal blocks that lie directly above the diagonal blocks. These interlayer edges are nondiagonal, because they connect nodes in one layer to different nodes in a neighboring layer. This formulation, which is connected mathematically [29] to matrix-iteration-based centrality measures for temporal networks [37–39], has been used to study time-dependent functional brain networks [111]. Multilayer networks with non-diagonal edges were also used in [112] to study disease spreading on temporal networks. Moreover, one can also choose to study multiplex and temporal networks without interlayer coupling by independently considering each layer in isolation.

Table 1

Summary of our mathematical notation for objects with different dimensionalities.

Typeface	Class	Dimensionality
\mathbb{M}	matrix	$NT \times NT$
\mathbf{M}	matrix	$N \times N$
\mathbf{M}	matrix	$T \times T$
\mathbf{w}	vector	$NT \times 1$
\mathbf{v}	vector	$N \times 1$
\mathbf{v}	vector	$T \times 1$
M_{ij}	scalar	1
v_i	scalar	1

3. Supracentrality Framework for Multiplex and Temporal Networks. We now present a supracentrality framework that provides a common mathematical foundation for eigenvector-based centralities for (layer-coupled) multiplex and temporal networks. In Sec. 3.1, we define supracentrality matrices. In Sec. 3.2, we define joint, marginal, and conditional centralities; and we prove their uniqueness and positivity under certain conditions. In Sec. 3.3, we provide a pedagogical example to illustrate these concepts. We summarize our key mathematical notation in Table 1. We use subscripts $i \in \mathcal{V}$ to enumerate nodes, subscripts $t \in \{1, \dots, T\}$ to enumerate layers, and subscripts $n \in \{1, \dots, NT\}$ to enumerate node-layer pairs.

3.1. Supracentrality Matrices. We first define a supracentrality matrix, in a way that generalizes the definition in [105], for networks that are either multiplex or temporal.

Definition 3.1 (Supracentrality Matrix). Let $\{\mathbf{C}^{(t)}\}$ be a set of T centrality matrices for a multilayer network whose layers have a common set $\mathcal{V} = \{1, \dots, N\}$ of nodes, and suppose that $C_{ij}^{(t)} \geq 0$. Let $\tilde{\mathbf{A}}$, with $\tilde{A}_{ij} \geq 0$, be a $T \times T$ interlayer-adjacency matrix that encodes the interlayer couplings. We define a family of supracentrality matrices $\mathbb{C}(\omega)$, which are parameterized by the interlayer-coupling strength $\omega \geq 0$, of the form

$$(3.1) \quad \mathbb{C}(\omega) = \hat{\mathbf{C}} + \omega \hat{\mathbf{A}} = \begin{bmatrix} \mathbf{C}^{(1)} & \mathbf{0} & \mathbf{0} & \dots \\ \mathbf{0} & \mathbf{C}^{(2)} & \mathbf{0} & \dots \\ \mathbf{0} & \mathbf{0} & \mathbf{C}^{(3)} & \ddots \\ \vdots & \vdots & \ddots & \ddots \end{bmatrix} + \omega \begin{bmatrix} \tilde{A}_{11}\mathbf{I} & \tilde{A}_{12}\mathbf{I} & \tilde{A}_{13}\mathbf{I} & \dots \\ \tilde{A}_{21}\mathbf{I} & \tilde{A}_{22}\mathbf{I} & \tilde{A}_{23}\mathbf{I} & \dots \\ \tilde{A}_{31}\mathbf{I} & \tilde{A}_{32} & \tilde{A}_{33}\mathbf{I} & \dots \\ \vdots & \vdots & \vdots & \ddots \end{bmatrix},$$

where $\hat{\mathbf{C}} = \text{diag}[\mathbf{C}^{(1)}, \dots, \mathbf{C}^{(T)}]$ and $\hat{\mathbf{A}} = \tilde{\mathbf{A}} \otimes \mathbf{I}$ denotes the Kronecker product of $\tilde{\mathbf{A}}$ and \mathbf{I} .

Remark 3.1. For layer t , the matrix $\mathbf{C}^{(t)}$ can represent any matrix whose dominant eigenvector is of interest. We focus on centrality matrices, such as those that are associated with eigenvector centrality (see Definition 2.3), hub and authority scores (see Definition 2.4), or PageRank (see Definition 2.5). Additionally, note that one can scale each $\mathbf{C}^{(t)}$ by a layer-specific weight. (Such a scaling benefit both multilayer community detection [79] and layer-averaged clique detection [74].) One can easily incorporate such weighting into Eq. (3.1) by redefining the centrality matrices $\{\mathbf{C}^{(t)}\}$ to include the weights.

The supracentrality matrix $\mathbb{C}(\omega)$ of size $NT \times NT$ encodes the effects of two distinct types of connections: the layer-specific centrality entries $\{C_{ij}^{(t)}\}$ in the diagonal blocks relate centralities between nodes within layer t , whereas entries in the off-diagonal blocks encode coupling between layers. The form $\hat{\mathbf{A}} = \tilde{\mathbf{A}} \otimes \mathbf{I}$ implements uniform and diagonal coupling: the matrix \mathbf{I} encodes diagonal coupling, and any two layers t and t' are uniformly coupled, because all interlayer edges between them have the identical weight $w\tilde{A}_{tt'}$. The choice of undirected, adjacent-in-time interlayer coupling (i.e., $\tilde{A}_{tt'} = 1$ if $|t - t'| = 1$ and $\tilde{A}_{tt'} = 0$ otherwise) recovers the supracentrality matrix that we studied in [105]. In the present paper, we generalize their notion of supracentrality matrices by using an interlayer-adjacency matrix $\tilde{\mathbf{A}}$, which allows one to implement a wide variety of interlayer coupling topologies. In the context of multiplex networks, we hypothesize that different choices for $\tilde{\mathbf{A}}$ will have different benefits. In the context of temporal networks, we will study (see Sec. 5.2) the effects of

letting $\tilde{\mathbf{A}}$ encode a directed, time-respecting chain with “layer” teleportation (see Eq. (5.1)), obtaining supracentrality results that we contrast with those in [105].

3.2. Joint, Marginal, and Conditional Centralities. The defining feature of eigenvector-based centrality measures is that one computes and studies a dominant eigenvector of a centrality matrix. Therefore, we study the right dominant eigenvalue equation

$$(3.2) \quad \mathbb{C}(\omega)\mathfrak{v}(\omega) = \lambda_{\max}(\omega)\mathfrak{v}(\omega),$$

where we interpret entries in the right dominant eigenvector $\mathfrak{v}(\omega)$ as centrality measures for the node-layer pairs $\{(i, t)\}$. The vector $\mathfrak{v}(\omega)$ has a block form: its first N entries encode the joint centralities for layer $t = 1$, its next N entries encode the joint centralities for layer $t = 2$, and so on. Therefore, as we now describe, it can be useful to reshape $\mathfrak{v}(\omega)$ into a matrix.

Following [105], we use the concepts of *joint*, *marginal*, and *conditional* centralities to develop our understanding of the importances of nodes and layers from the computed values of $\mathfrak{v}(\omega)$.

Definition 3.2 (Joint Centrality of a Node-Layer Pair [105]). Let $\mathbb{C}(\omega)$ be a supracentrality matrix given by Definition 3.1, and let $\mathfrak{v}(\omega)$ be its dominant right eigenvector. We encode the joint centrality of node i in layer t via the $N \times T$ matrix $\mathbf{W}(\omega)$ with entries

$$(3.3) \quad W_{it}(\omega) = \mathfrak{v}_{N(t-1)+i}(\omega).$$

Remark 3.2. We refer to $W_{it}(\omega)$ as a “joint centrality” because it reflects the importance both of node i and of layer t .

Definition 3.3 (Marginal Centralities of Nodes and Layers [105]). Let $\mathbf{W}(\omega)$ encode the joint centralities given by Definition 3.2. We define the marginal layer centrality (MLC) and marginal node centrality (MNC), respectively, by

$$(3.4) \quad x_t(\omega) = \sum_i W_{it}(\omega), \quad \hat{x}_i(\omega) = \sum_t W_{it}(\omega).$$

Definition 3.4 (Conditional Centralities of Nodes and Layers [105]). Let $\{W_{it}(\omega)\}$ be the joint centralities given by Definition 3.2, and let $\{x_t(\omega)\}$ and $\{\hat{x}_i(\omega)\}$, respectively, be the marginal node and layer centralities given by Definition 3.3. We define the conditional centralities of nodes and layers by

$$(3.5) \quad Z_{it}(\omega) = W_{it}(\omega)/x_t(\omega), \quad \hat{Z}_{it}(\omega) = W_{it}(\omega)/\hat{x}_i(\omega),$$

where $Z_{it}(\omega)$ gives the centrality of node i conditioned on layer t and $\hat{Z}_{it}(\omega)$ gives the centrality of layer t conditioned on node i .

Note that $Z_{it}(\omega)$ indicates the importance of node i relative to other nodes in layer t , in contrast with the joint node-layer centrality $W_{it}(\omega)$, which reflects the importance of node-layer pair (i, t) relative to all node-layer pairs.

We now present a new theorem that ensures the uniqueness and positivity of the above supracentralities.

Theorem 3.5 (Uniqueness and Positivity of Supracentralities). *Let $\mathbb{C}(\omega)$ be a supracentrality matrix given by Eq. (3.1). Additionally, suppose that $\tilde{\mathbf{A}}$ is an adjacency matrix for a strongly connected graph; and suppose that the sum $\sum_t \mathbf{C}^{(t)}$ is an irreducible nonnegative matrix. It then follows that $\mathbb{C}(\omega)$ is irreducible, nonnegative, and has a simple largest positive eigenvalue $\lambda_{\max}(\omega)$, with corresponding left eigenvector $\mathbf{u}(\omega)$ and right eigenvector $\mathbf{v}(\omega)$, which are unique and consist of positive entries. Moreover, the centralities $\{W_{it}(\omega)\}$, $\{x_i(\omega)\}$, $\{\hat{x}_t(\omega)\}$, $\{Z_{it}(\omega)\}$, and $\{\hat{Z}_{it}(\omega)\}$ are positive and well-defined. If we also assume that $\mathbb{C}(\omega)$ is aperiodic, then it follows that $\lambda_{\max}(\omega)$ is a unique dominant eigenvalue.*

Proof. See Appendix A. ■

3.3. Pedagogical Example Illustrating Interlayer-Coupling Regimes. In Fig. 2, we illustrate the concepts of joint and marginal centralities for the network in Fig. 1(a). The multiplex network has $N = 4$ nodes and $T = 6$ layers, and we study the interlayer-adjacency matrix $\tilde{\mathbf{A}}$ that we showed in the inset of Fig. 1(a). Specifically, we set $\tilde{A}_{tt'} = 1$ for all depicted interlayer couplings, except for the coupling of layers 3 and 4, for which we set $\tilde{A}_{34} = \tilde{A}_{43} = 0.01$. With this weighting, the interlayer-coupling network associated with $\tilde{\mathbf{A}}$ has two natural communities of densely-connected nodes.

		layer index						MNC
		1	2	3	4	5	6	
node index	1	0.1615	0.1578	0.1554	0.1930	0.1923	0.1925	1.0524
	2	0.0961	0.0959	0.0958	0.3008	0.3064	0.3123	1.2072
	3	0.1468	0.1504	0.1511	0.1930	0.1923	0.1925	1.0260
	4	0.1188	0.1185	0.1225	0.3131	0.3068	0.3009	1.2807
MLC		0.5231	0.5226	0.5248	0.9999	0.9978	0.9981	

Figure 2. Joint node-layer centralities $\{W_{it}(\omega)\}$ given by Definition 3.2 (white cells), with corresponding marginal layer centralities (MLC) $\{x_t(\omega)\}$ and marginal node centralities (MNC) $\{\hat{x}_i(\omega)\}$ given by Definition 3.3 (gray cells), for the multiplex network in Fig. 1(a). These results are for diagonally and uniformly coupled (i.e., layer-coupled) eigenvector centralities in which the layers' centrality matrices are given by Definition 2.3 with $\omega = 1$.

For this experiment (and our other experiments), we typically find that conditional centrality provides the most useful insights. In Fig. 3(a), we plot the conditional centralities $\{Z_{it}(\omega)\}$ of node-layers for three different choices of ω . These choices represent three centrality regimes (which we illustrate in Fig. 3(b)) that we observe by exploring centralities across a range of ω values. In the top two panels of Fig. 3(b), we plot the MNC and MLC values versus ω . In the bottom panel, we quantify the sensitivity of the joint and conditional centralities to perturbations of ω . Specifically, we consider ω in the interval $[10^{-2}, 10^4]$ discretized by $\omega_s = 10^{-2+0.2s}$ for $s \in \{0, \dots, 30\}$. We plot the stepwise magnitudes of the change $\|\mathbf{W}(\omega_s) - \mathbf{W}(\omega_{s-1})\|_F$ of the joint centralities and the change $\|\mathbf{Z}(\omega_s) - \mathbf{Z}(\omega_{s-1})\|_F$ of the conditional centralities, where $\|\cdot\|_F$ denotes the Frobenius norm. We identify three regimes for which the conditional centralities are robust. (See the shaded regions in the bottom panel

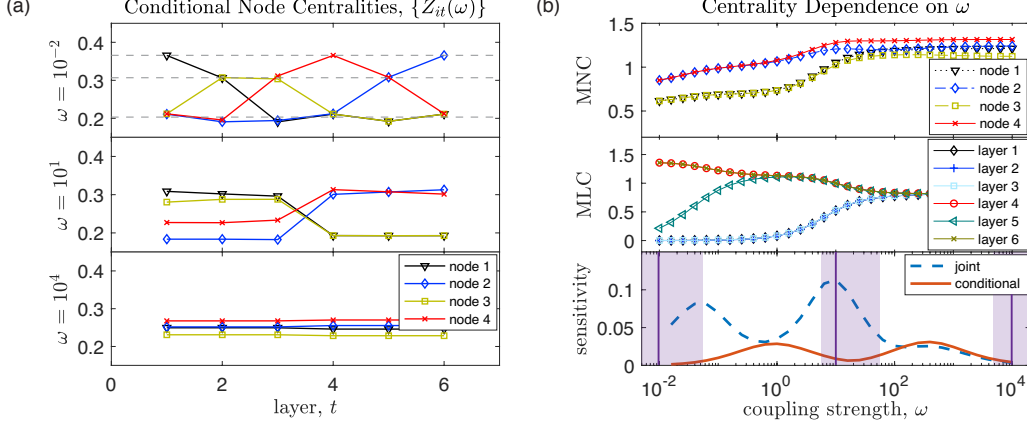


Figure 3. Eigenvector centralities (see Definition 2.3) for the uniformly and diagonally coupled multilayer network with interlayer-adjacency matrix $\tilde{\mathbf{A}}$ given by $\tilde{A}_{tt'} = 1$, except for the pair $(t, t') = (3, 4)$ (for which $\tilde{A}_{34} = \tilde{A}_{43} = 0.01$), for the coupled layers in Fig. 1(a). (a) Conditional node centralities $\{Z_{it}(\omega)\}$ versus t for $\omega \in \{10^{-2}, 10, 10^4\}$. The horizontal dashed lines in the top panel highlight that $\{Z_{it}(\omega)\}$ values correlate with intralayer node degrees $d_i^{(t)} = \sum_j A_{ij}^{(t)}$. The conditional node centralities are $Z_{it}(\omega) \approx 0.3656$ for $d_i^{(t)} = 3$, $Z_{it}(\omega) \approx 0.3096$ for $d_i^{(t)} = 2$, and $Z_{it}(\omega) \approx 0.2021$ for $d_i^{(t)} = 1$. (b) MNC and MLC versus ω on the interval $[10^{-2}, 10^4]$ discretized by $\omega_s = 10^{-2+0.2s}$ for $s \in \{0, \dots, 30\}$. The bottom panel depicts a measure for the sensitivity of centralities with respect to ω . The blue dashed curve indicates the stepwise magnitude of change, $\|\mathbf{W}(\omega_s) - \mathbf{W}(\omega_{s-1})\|_F$, for the joint centralities, and the solid red curve indicates the change $\|\mathbf{Z}(\omega_s) - \mathbf{Z}(\omega_{s-1})\|_F$ for the conditional centralities. The shaded regions highlight that, because the curve representing $\|\mathbf{Z}(\omega_s) - \mathbf{Z}(\omega_{s-1})\|_F$ is bimodal, there are three ranges of ω that are separated by two peaks. The three vertical lines in panel (b) indicate the values of ω from panel (a).

of Fig. 3(b).) That is, the peaks in Fig. 3(b) indicate values of ω where conditional centralities are most sensitive to perturbations of ω ; other choices for ω are more robust to a perturbation of ω . Interestingly, the peaks and troughs for the curves for $\|\mathbf{W}(\omega_s) - \mathbf{W}(\omega_{s-1})\|_F$ and $\|\mathbf{Z}(\omega_s) - \mathbf{Z}(\omega_{s-1})\|_F$ do not coincide. We focus on robust values of $\mathbf{Z}(\omega)$, because we generally find conditional centrality to provide the most interpretable and insightful results (See Sec. 3.2 below and Sec. 5 in [105].)

We summarize these three regimes as follows:

- **Weak-Coupling Regime.** The top panel of Fig. 3(a), at $\omega = 10^{-2}$, represents a regime in which conditional centralities resemble the centralities of uncoupled layers as $\omega \rightarrow 0^+$. In this example, we observe that the conditional centralities correlate strongly with intralayer degrees ($d_i^{(t)} = \sum_j A_{ij}^{(t)}$). Specifically, as we indicate with the horizontal dashed lines, the conditional centralities approximately equal one of three values: $Z_{it} \approx 0.3656$ for $d_i^{(t)} = 3$; $Z_{it} \approx 0.3096$ for $d_i^{(t)} = 2$; and $Z_{it} \approx 0.2021$ for $d_i^{(t)} = 1$. We analyze the $\omega \rightarrow 0^+$ limit in Sec. 4.1.
- **Strong-Coupling Regime.** The bottom panel of Fig. 3(a), at $\omega = 10^4$, represents a regime in which the conditional centralities approach the centralities of a layer-aggregated centrality matrix as $\omega \rightarrow \infty$. In this regime, the conditional centralities limit to a value $Z_{it} \rightarrow \alpha_i$ for each i that is constant across the layers. We analyze the $\omega \rightarrow \infty$ limit in Sec. 4.2.
- **Intermediate-Coupling Regime.** The middle panel of Fig. 3(a) represents an intermediate regime with $\omega = 10$, which is a value of ω that lies between the locations of the two peaks for the bimodal curve $\|\mathbf{Z}(\omega_s) - \mathbf{Z}(\omega_{s-1})\|_F$ that we show in Fig. 3(b). For $\omega = 10$, we observe

two subsets of Z_{it} conditional centrality values: those for layers $t \in \{1, 2, 3\}$ are very similar to each other; and those for layers $t \in \{4, 5, 6\}$ are also similar to each other. This pattern arises directly from the layer-coupling scheme in Fig. 1(a), where these two sets of layers correspond to two communities for the interlayer-adjacency matrix. (Recall that the coupling between layers 3 and 4 is 100 times weaker than the other couplings.) In Sec. SM1 of the Supplementary Material, we show that the curve $\|\mathbf{Z}(\omega_s) - \mathbf{Z}(\omega_{s-1})\|_F$ becomes unimodal as one increases the coupling weight between layers 3 and 4.

We classify the strong and weak regimes by considering whether or not the observed supracentralities are strongly correlated with those of either asymptotic limit (i.e., either $\omega \rightarrow 0^+$ or $\omega \rightarrow \infty$). The intermediate regime arises from an interplay between the topologies and edge weights of both the layers and the interlayer couplings, so these multilayer centralities provide insights that cannot be observed by studying the network layers in isolation or in aggregate. This example also illustrates that it is important to explore various coupling strengths ω and various interlayer-adjacency matrices \mathbf{A} to identify supracentralities that are appropriate for a given application. See [102] for our MATLAB code that computes supracentralities and reproduces Fig. 3 and our other experiments in this paper.

4. Limiting Behavior for Weak and Strong Coupling. We construct singular perturbation expansions to analyze the limiting behaviors of Eq. (3.2) when the interlayer-coupling strength ω is very small (i.e., layer decoupling) or very large (i.e., layer aggregation). These results provide insights into our supracentrality framework and can aid in the selection of appropriate parameter choices.

4.1. Layer Decoupling in the Weak-Coupling Limit. We first give a general result for the $\omega \rightarrow 0^+$ limit for all eigenvalues and eigenvectors of $\mathbb{C}(\omega)$. We did not study this limit in our previous work [105] on temporal centralities.

Theorem 4.1 (Layer Decoupling as $\omega \rightarrow 0^+$). *Assume that each layer's $N \times N$ centrality matrix $\mathbf{C}^{(t)}$ is diagonalizable, and let $\{\mu_i^{(t)}\}$, $\{\mathbf{u}^{(i,t)}\}$ and $\{\mathbf{v}^{(i,t)}\}$ denote its N eigenvalues and the corresponding left and right eigenvectors, respectively, for $i \in \mathcal{V} = \{1, \dots, N\}$ and $t \in \{1, \dots, T\}$. Let $\mathbb{C}(\omega)$ denote a supracentrality matrix given by Eq. (3.1), and let $\{\lambda_n(\omega)\}$ denote its NT eigenvalues, with corresponding left and right eigenvectors $\mathbf{u}^{(n)}(\omega)$ and $\mathbf{v}^{(n)}(\omega)$, respectively, and $n \in \{1, \dots, NT\}$. In the limit $\omega \rightarrow 0^+$, we have $\mathbb{C}(\omega) \rightarrow \hat{\mathbb{C}} = \text{diag}[\mathbf{C}^{(1)}, \dots, \mathbf{C}^{(T)}]$ and $\{\lambda_n(\omega)\} \rightarrow \cup_t \{\mu_i^{(t)}\}$. The limiting associated left and right eigenvectors $\mathbf{u}^{(n)}(\omega)$ and $\mathbf{v}^{(n)}(\omega)$ are determined by functions of the eigenvectors $\{\mathbf{u}^{(i,t)}\}$ and $\{\mathbf{v}^{(i,t)}\}$, respectively. There are two cases, which depend on the sets of eigenvalues.*

- (1) *When the eigenvalues $\{\mu_i^{(t)}\}$ of $\mathbf{C}^{(t)}$ are simple and differ across layers (i.e., when $\{\mu_i^{(t)}\} \cap \{\mu_i^{(t')}\} = \emptyset$ for $t \neq t'$) there is a one-to-one correspondence between $\{\mu_i^{(t)}\}$ and $\{\lambda_n(0^+)\}$. The limiting eigenvalues of $\mathbb{C}(0^+)$ are then simple and have corresponding eigenvectors $\mathbf{u}^{(n)}(\omega) \rightarrow \mathbf{u}^{(i,t)} = \mathbf{e}^{(t)} \otimes \mathbf{u}^{(i,t)}$ and $\mathbf{v}^{(n)}(\omega) \rightarrow \mathbf{v}^{(i,t)} = \mathbf{e}^{(t)} \otimes \mathbf{v}^{(i,t)}$, where $\mathbf{e}^{(t)}$ denotes a length- T unit vector that consists of 0s in all entries except for the t -th entry, which is a 1. Therefore, the vectors $\mathbf{u}^{(i,t)}$ and $\mathbf{v}^{(i,t)}$ consist of 0s except in the t -th block, where they consist of $\mathbf{u}^{(i,t)}$ in the former case and $\mathbf{v}^{(i,t)}$ in the latter. (See the paragraph after Eq. (3.2) for a description of a block vector.)*
- (2) *When there are repeated eigenvalues, such that there exists a set $\mathcal{P} = \{(i,t) | \mu_i^{(t)} = \lambda_n\}$ with cardinality $P = |\mathcal{P}|$, each unique eigenvalue λ_n of $\mathbb{C}(0)$ has P -dimensional eigenspaces that are spanned by the left and right eigenvectors, $\{\mathbf{u}^{(i,t)}\}$ and $\{\mathbf{v}^{(i,t)}\}$, that are associated with λ_n .*

Proof. See Appendix B. ■

We now present a key result for the left and right dominant eigenvectors of $\mathbb{C}(\omega)$.

Theorem 4.2 (Weak-Coupling Limit of Dominant Eigenvectors). *Let $\mathbf{u}^{(1)}(\omega)$ and $\mathbf{v}^{(1)}(\omega)$, respectively, be the dominant left and right eigenvectors of a supracentrality matrix under the assumptions of Thms. 3.5 and 4.1. Additionally, let $\mathcal{P} = \{t : \mu_1^{(t)} = \lambda_{\max}(0)\}$ denote the set of indices associated with*

the eigenvalues of $\mathbf{C}^{(t)}$ that equal the largest eigenvalue $\lambda_{\max}(0)$ of $\mathbb{C}(0)$. We assume that each layer's dominant eigenvalue $\mu_1^{(t)}$ is simple. It then follows that the $\omega \rightarrow 0^+$ limits of $\mathbf{u}^{(1)}(\omega)$ and $\mathbf{v}^{(1)}(\omega)$ are

$$(4.1) \quad \mathbf{v}^{(1)}(\omega) \rightarrow \sum_{t \in \mathcal{P}} \alpha_t \mathbf{v}^{(1,t)}, \quad \mathbf{u}^{(1)}(\omega) \rightarrow \sum_{t \in \mathcal{P}} \beta_t \mathbf{u}^{(1,t)},$$

where the vectors $\boldsymbol{\alpha} = [\alpha_1, \dots, \alpha_T]^T$ and $\boldsymbol{\beta} = [\beta_1, \dots, \beta_T]^T$, which have nonnegative entries that satisfy $\sum_t \alpha_t^2 = \sum_t \beta_t^2 = 1$, are unique solutions to

$$(4.2) \quad \mathbf{X}\boldsymbol{\alpha} = \lambda_1 \boldsymbol{\alpha}, \quad \mathbf{X}^T \boldsymbol{\beta} = \lambda_1 \boldsymbol{\beta},$$

where λ_1 is an eigenvalue that needs to be determined and the entries of \mathbf{X} are

$$(4.3) \quad X_{tt'} = \tilde{A}_{t,t'} \frac{\langle \mathbf{u}^{(1,t)}, \mathbf{v}^{(1,t')} \rangle}{\langle \mathbf{u}^{(1,t)}, \mathbf{v}^{(1,t)} \rangle} \chi(t) \chi(t'),$$

where $\chi(t) = \sum_{t' \in \mathcal{P}} \delta_{tt'}$ is an indicator function, with $\chi(t) = 1$ if $t \in \mathcal{P}$ and $\chi(t) = 0$ otherwise.

Proof. See Appendix C. ■

It is worthwhile to consider Thm. 4.2 under various restrictions on the centrality matrices. These yield three useful corollaries.

When the layers' centrality matrices all have the same spectral radius, as is the case for PageRank matrices (because they correspond to transition matrices of Markov chains) or if one rescales the centrality matrices to have the same spectral radius, then the limiting behavior simplifies.

Corollary 4.3 (Weak-Coupling Limit for Spectral-Radii-Equivalent Centrality Matrices). *Under the assumptions of Thm. 4.2 and assuming that all centrality matrices have the same spectral radius (i.e., $\lambda_{\max} = \mu_1^{(t)}$ for all t), then $\mathcal{P} = \{1, \dots, T\}$ and $\chi(t) = 1$; and Eq. (4.3) takes the form*

$$(4.4) \quad X_{tt'} = \tilde{A}_{t,t'} \frac{\langle \mathbf{u}^{(1,t)}, \mathbf{v}^{(1,t')} \rangle}{\langle \mathbf{u}^{(1,t)}, \mathbf{v}^{(1,t)} \rangle}.$$

When the layers' centrality matrices are symmetric, which is the case for hub/authority matrices and for symmetric adjacency matrices, the limiting behavior also simplifies.

Corollary 4.4 (Weak-Coupling Limit for Symmetric Centrality Matrices). *Under the assumptions of Thm. 4.2 and assuming that all centrality matrices are symmetric, then $\mathbf{u}^{(1,t)} = \mathbf{v}^{(1,t')}$ and Eq. (4.3) takes the form*

$$(4.5) \quad X_{tt'} = \tilde{A}_{t,t'} \chi(t) \chi(t').$$

When the centrality matrix of a single layer has the largest spectral radius, which one often expects to occur for adjacency matrices and hub/authority matrices (unless the network layers have symmetries that yield repeated spectral radii across layers), the limiting behavior of the eigenvector is that it localizes onto a single dominating layer.

Corollary 4.5 (Weak-Coupling-Induced Eigenvector Localization onto a Dominating Layer). *Under the assumptions of Thm. 4.2 and assuming that one single layer has a spectral radius that is larger than all others (i.e., $\lambda_{\max} = \mu_1^{(t)}$ for a single layer $t = t^*$), then as $\omega \rightarrow 0^+$, we have that*

$$(4.6) \quad \mathbf{v}(\omega) \rightarrow \mathbf{v}^{(1,t^*)}, \quad \mathbf{u}(\omega) \rightarrow \mathbf{u}^{(1,t^*)}.$$

Understanding whether or not the dominant eigenvector localizes onto a single layer, onto several layers (i.e., as given by the function $\chi(t)$), or does not localize has significant practical consequences. In some situations, it can be appropriate to allow eigenvector localization [81], whereas it can be beneficial to avoid localization in others [69]. Our results in this subsection characterize localization in the weak-coupling limit and are useful for practitioners to make better-informed choices about which centrality matrices to use.

4.2. Layer Aggregation in the Strong-Coupling Limit. We now study Eq. (3.2) in the limit as $\omega \rightarrow \infty$ (or, equivalently, as $\epsilon := \omega^{-1} \rightarrow 0^+$). The results of this subsection significantly generalize those of [105], where we assumed that $\tilde{\mathbf{A}}$ encodes adjacent-in-time coupling. In the present discussion, by contrast, we allow $\tilde{\mathbf{A}}$ to be from a much more general class of matrices, including asymmetric matrices that encode directed interlayer couplings.

Consider the scaled supracentrality matrix

$$(4.7) \quad \tilde{\mathbb{C}}(\epsilon) = \epsilon \mathbb{C}(\epsilon^{-1}) = \epsilon \hat{\mathbb{C}} + \hat{\mathbb{A}},$$

which has eigenvectors $\tilde{\mathbf{u}}(\epsilon)$ and $\tilde{\mathbf{v}}(\epsilon)$ that are identical to those of $\mathbb{C}(\omega)$ (specifically, $\tilde{\mathbf{u}}(\epsilon) = \mathbf{u}(\epsilon^{-1})$ and $\tilde{\mathbf{v}}(\epsilon) = \mathbf{v}(\epsilon^{-1})$). Its eigenvalues $\{\tilde{\lambda}_i\}$ are scaled by ϵ ; specifically, $\tilde{\lambda}_i(\epsilon) = \epsilon \lambda_i(\epsilon^{-1})$.

To facilitate our presentation, we define a permutation operator for $NT \times NT$ matrices.

Definition 4.6 (Node-Layer-Reordering Stride Permutation). *The matrix \mathbb{P} is a T -stride permutation matrix of size $NT \times NT$ if it has entries that take the form [34]*

$$(4.8) \quad [\mathbb{P}]_{kl} = \begin{cases} 1, & l = [k/N] + T[(k-1) \bmod N], \\ 0, & \text{otherwise.} \end{cases}$$

Therefore, $(\tilde{\mathbf{A}} \otimes \mathbf{I}) = \mathbb{P}(\mathbf{I} \otimes \tilde{\mathbf{A}})\mathbb{P}^T$.

Remark 4.1. *The stride-permutation matrix is unitary, and it simply changes the ordering of node-layer pairs. That is, a supracentrality matrix has entries that are ordered first by node i and then by layer t (i.e., $(i, t) = (1, 1), (2, 1), (3, 1), \dots$); after the permutation, the entries are ordered first by layer t and then by node i (i.e., $(i, t) = (1, 1), (1, 2), (1, 3), \dots$). We note in passing that this permutation is one type of graph isomorphism [55].*

We now present our main findings for the strong-coupling regime.

Theorem 4.7 (Singularity at Infinite Coupling). *Assume that the interlayer-adjacency matrix $\tilde{\mathbf{A}}$ is diagonalizable and has T distinct eigenvalues. Let $\{\tilde{\mu}_t\}$ denote its T eigenvalues, and let $\{\tilde{\mathbf{u}}^{(t)}\}$ and $\{\tilde{\mathbf{v}}^{(t)}\}$, respectively, be the corresponding left and right eigenvectors. We assume that the eigenvalues are simple, and we order them such that $\tilde{\mu}_1$ is the largest eigenvalue. We also let \mathbb{P} denote the stride permutation matrix from Eq. (4.8).*

For $\epsilon = 0$, the spectrum $\{\tilde{\lambda}_i(0)\}$ of the supracentrality matrix $\mathbb{C}(\epsilon)$ given by Eq. (4.7) is identical to that of $\tilde{\mathbf{A}}$. Each eigenvalue $\lambda_i(0) = \tilde{\mu}_t$ has multiplicity N , and its associated N -dimensional left and right eigenspaces are spanned by eigenvectors $\tilde{\mathbf{u}}^{(t)}$ and $\tilde{\mathbf{v}}^{(t)}$, respectively, with the general form

$$(4.9) \quad \tilde{\mathbf{v}}^{(t)} = \sum_j \tilde{\alpha}_{tj} \mathbb{P} \tilde{\mathbf{v}}^{(t,j)}, \quad \tilde{\mathbf{u}}^{(t)} = \sum_j \tilde{\beta}_{tj} \mathbb{P} \tilde{\mathbf{u}}^{(t,j)},$$

where the constants $\{\tilde{\alpha}_{tj}\}$ and $\{\tilde{\beta}_{tj}\}$ must satisfy $\sum_j \tilde{\alpha}_{tj}^2 = \sum_j \tilde{\beta}_{tj}^2 = 1$ to ensure that $\|\tilde{\mathbf{u}}^{(t)}\|_2 = \|\tilde{\mathbf{v}}^{(t)}\|_2 = 1$. The associated length- NT vectors are given by $\tilde{\mathbf{v}}^{(t,j)} = \tilde{\mathbf{e}}^{(j)} \otimes \mathbf{v}^{(t)}$ and $\tilde{\mathbf{u}}^{(t,j)} = \tilde{\mathbf{e}}^{(j)} \otimes \mathbf{u}^{(t)}$, where $\tilde{\mathbf{e}}^{(j)}$ is a length- N unit vector that consists of 0s except for entry j , which is 1. Therefore, the vectors $\tilde{\mathbf{u}}^{(t,j)}$ and $\tilde{\mathbf{v}}^{(t,j)}$ consist of 0s, except the j -th block of size T , which consists of an eigenvector of $\tilde{\mathbf{A}}$.

Proof. See Appendix D. ■

Remark 4.2. *It is straightforward to also obtain the general form of eigenvectors for eigenvalues $\{\mu_t\}$ whose multiplicity is more than 1. For example, if the eigenvalue $\tilde{\mu}_t$ of $\tilde{\mathbf{A}}$ has multiplicity q , then $\tilde{\lambda}_i(0) = \tilde{\mu}_t$ has multiplicity qN for the matrix $\mathbb{C}(0)$. However, the notation becomes slightly more cumbersome, and we will not study such cases in this paper.*

Theorem 4.8 (Strong-Coupling Limit of Dominant Eigenvectors). *Let $\tilde{\mu}_1$ denote the dominant eigenvalue (which we assume to be simple) of the interlayer-adjacency matrix $\tilde{\mathbf{A}}$, and let $\tilde{\mathbf{u}}^{(1)}$ and $\tilde{\mathbf{v}}^{(1)}$ be its associated left and right eigenvectors. We assume that the constraints of Thm. 3.5 are satisfied, such that the supracentrality matrix $\mathbb{C}(\epsilon)$ given by Eq. (3.1) is nonnegative, irreducible, and aperiodic. It then follows that the dominant eigenvalue $\tilde{\lambda}_{\max}(\epsilon)$ and the associated eigenvectors $\tilde{\mathbf{u}}^{(1)}(\epsilon)$ and $\tilde{\mathbf{v}}^{(1)}(\epsilon)$ of $\mathbb{C}(\epsilon)$ converge as $\epsilon \rightarrow 0^+$ as follows:*

$$(4.10) \quad \tilde{\lambda}_{\max}(\epsilon) \rightarrow \tilde{\mu}_1, \quad \tilde{\mathbf{v}}^{(1)}(\epsilon) \rightarrow \sum_j \tilde{\alpha}_j \mathbb{P} \tilde{\mathbf{v}}^{(1,j)}, \quad \tilde{\mathbf{u}}^{(1)}(\epsilon) \rightarrow \sum_j \tilde{\beta}_j \mathbb{P} \tilde{\mathbf{u}}^{(1,j)},$$

where \mathbb{P} is the stride permutation from Eq. (4.8), the vectors $\tilde{\mathbf{u}}^{(1,j)}$ and $\tilde{\mathbf{v}}^{(1,j)}$ are defined in Thm. 4.7, and the constants $\{\tilde{\beta}_i\}$ and $\{\tilde{\alpha}_i\}$ solve the dominant eigenvalue equations

$$(4.11) \quad \tilde{\mathbf{X}} \tilde{\boldsymbol{\alpha}} = \tilde{\mu}_1 \tilde{\boldsymbol{\alpha}}, \quad \tilde{\mathbf{X}}^T \tilde{\boldsymbol{\beta}} = \tilde{\mu}_1 \tilde{\boldsymbol{\beta}},$$

where

$$(4.12) \quad \tilde{X}_{ij} = \sum_t C_{ij}^{(t)} \frac{\tilde{u}_t^{(1)} \tilde{v}_t^{(1)}}{\langle \tilde{\mathbf{u}}^{(1)}, \tilde{\mathbf{v}}^{(1)} \rangle}.$$

Proof. See Appendix E. ■

Equation (4.12) indicates that the strong-coupling limit effectively aggregates the centrality matrices $\{\mathbf{C}^{(t)}\}$ across time via a weighted average, with weights that depend on the left and right dominant eigenvectors of the interlayer-adjacency matrix $\tilde{\mathbf{A}}$. This result generalizes Eq. (4.13) of [105], which assumed that $\tilde{\mathbf{A}}$ is symmetric (so that $\tilde{u}_t^{(1)} = \tilde{v}_t^{(1)}$). We recover the result in [105] with the following corollary.

Corollary 4.9 (Strong-Coupling Limit of Eigenvector-Based Centralities for Multilayer Networks with Adjacent-in-Time, Uniform, and Diagonal Coupling [105]). *For undirected, adjacent-in-time interlayer coupling (i.e., $\tilde{A}_{tt'} = 1$ for $|t - t'| = 1$ and $\tilde{A}_{tt'} = 0$ otherwise), the $\epsilon \rightarrow 0^+$ limit of the largest eigenvalue is $\tilde{\lambda}_1(\epsilon) \rightarrow 2 \cos\left(\frac{\pi}{T+1}\right)$; and, as $\epsilon \rightarrow 0^+$, the dominant left and right eigenvectors satisfy Eqs. (4.10)–(4.11), with*

$$\tilde{\mathbf{X}} = \sum_t \mathbf{C}^{(t)} \frac{\sin^2\left(\frac{\pi t}{T+1}\right)}{\sum_{t=1}^T \sin^2\left(\frac{\pi t}{T+1}\right)}.$$

Corollary 4.10 (Strong-Coupling Limit of Eigenvector-Based Centralities for Multilayer Networks with All-to-All, Uniform, and Diagonal Coupling). *For all-to-all coupling (without self edges), $\tilde{\mathbf{A}} = \mathbf{1}\mathbf{1}^T$; the $\epsilon \rightarrow 0^+$ limit of the largest eigenvalue is $\tilde{\lambda}_{\max}(\epsilon) \rightarrow \tilde{\mu}_1 = N$; and as $\epsilon \rightarrow 0^+$, the dominant left and right eigenvectors satisfy Eqs. (4.10)–(4.11), with $\tilde{\mathbf{X}} = T^{-1} \sum_t \mathbf{C}^{(t)}$.*

Proof. In this case, the largest eigenvalue of $\tilde{\mathbf{A}}$ is $\mu_1 = N$, and the left and right dominant eigenvectors have the same value in each component, with entries $u_t^{(1)} = v_t^{(1)} = T^{-1/2}$. ■

Corollary 4.11 (Strong-Coupling Limit of Eigenvector-Based Centralities for Multilayer Networks with Rank-1, Uniform, and Diagonal Coupling). *For a rank-1 interlayer-adjacency matrix, $\tilde{\mathbf{A}} = \tilde{\mathbf{w}}\tilde{\mathbf{w}}^T$, the $\epsilon \rightarrow 0^+$ limit of the largest eigenvalue is $\tilde{\lambda}_{\max}(\epsilon) \rightarrow 1$; and, as $\epsilon \rightarrow 0^+$, the dominant left and right eigenvectors satisfy Eqs. (4.10)–(4.11), with $\tilde{\mathbf{X}} = \sum_t \mathbf{C}^{(t)} \tilde{\mathbf{w}}_t^2$.*

Proof. This follows from the fact that the largest eigenvalue of $\tilde{\mathbf{A}}$ is $\tilde{\mu}_1 = 1$, with associated eigenvectors $\tilde{u}_t^{(1)} = \tilde{v}_t^{(1)} = \tilde{w}_t$. ■

5. Case Studies with Empirical Data. We now apply our supracentrality framework to study two data sets. In Sec. 5.1, we examine a multiplex network that encodes flight patterns between European airports, with layers representing different airline companies [13]. In Sec. 5.2, we examine a temporal network that encodes the exchange of mathematicians between mathematical-sciences doctoral programs in the United States [105]. These experiments explore different interlayer-coupling strengths and topologies; and they illustrate strategies for how to flexibly apply our supracentrality framework to diverse applications.

5.1. European Airport Rankings in a Multiplex Airline Network [13]. We first apply our supracentrality framework to study the importances of European airports using an empirical multiplex network of the flight patterns for $T = 37$ airline companies [13]. See Table SM1 in the Supplementary Material for a list of the airline companies and the number of edges and spectral radii of the adjacency matrices that correspond to their associated layers. See Fig. SM2 in the Supplementary Material for a map of the airports and a visualization of the network layers that have the most edges. The network's nodes represent European airports; we consider only the $N = 417$ nodes in the largest connected component of the network that is associated with the sum of the layers' adjacency matrices. We couple the layers using all-to-all coupling (so that $\tilde{\mathbf{A}} = \mathbf{1}\mathbf{1}^T$), and we calculate eigenvector supracentralities with the centrality matrices from Definition 2.3.

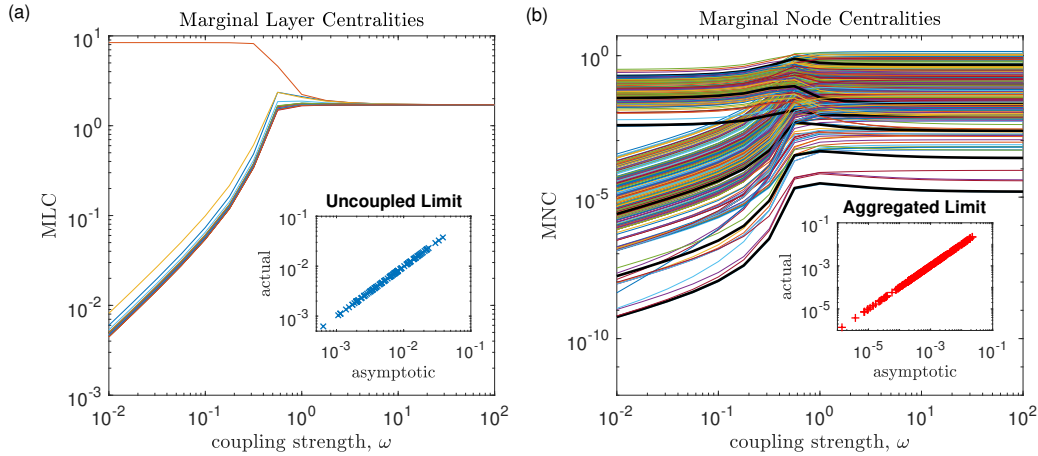


Figure 4. Marginal layer centralities (MLCs) and marginal node centralities (MNCs) for a multiplex European airline transportation network of flight patterns for 37 airlines [13]. We couple the layers with all-to-all coupling and examine $\omega \in [10^{-2}, 10^2]$. The insets in panels (a) and (b) compare observed conditional node centralities for $\omega = 10^{-2}$ and $\omega = 10^2$, respectively, to the asymptotic values from Thms. 4.2 and 4.8.

For each airport, we compute the joint, marginal, and conditional centralities for a range of coupling strengths ω . In Fig. 4, we plot the MLCs and MNCs (see Definition 3.3). In Fig. 4(a), we see that for large ω , all layers have similar importances; by contrast, for small ω , one layer is much more important, due to the eigenvector localization phenomenon that we described in Cor. 4.5. Specifically, the layer that represents Ryanair dominates for small ω , as its adjacency matrix has the largest spectral radius. (It also has the largest number of edges.) A previous investigation of multilayer centralities in this data set [87] also identified Ryanair as the most important layer.

The insets in Fig. 4 give the conditional centralities of nodes for $\omega = 10^{-2}$ (in panel (a)) and $\omega = 10^2$ (in panel (b)) versus the asymptotic values in the associated limits for $\omega \rightarrow 0^+$ (see Thm. 4.2) and $\omega \rightarrow \infty$ (see Thm. 4.8), demonstrating that they are in excellent agreement. One can also observe in Fig. 4(b) that there is not a simple transition between these two limits. Specifically, the thick black

curves highlight a few airports whose marginal node centralities have a peak for intermediate values of ω . That is, these airports are more important if one considers the airline network as a multiplex network than if one considers the layers in isolation or in aggregate.

Table 2

European airports with the largest MNCs for coupling strengths ω correspond to the regimes of weak, intermediate, and strong coupling. We give the results of our computations of eigenvector supracentralities with all-to-all, uniform, and diagonal coupling between layers. We identify each airport by its International Civil Aviation Organization (ICAO) code.

Rank	$\omega = 0.01$		$\omega = 1$		$\omega = 100$	
	Airport	MNC	Airport	MNC	Airport	MNC
1	EGSS	0.329	LEMD	1.379	EHAM	1.406
2	EIDW	0.286	EHAM	1.296	LEMD	1.400
3	LIME	0.254	LEBL	1.257	LIRF	1.206
4	EBCI	0.201	EDDM	1.171	LOWW	1.198
5	LEMD	0.193	LIRF	1.150	LEBL	1.193
6	LEAL	0.190	EDDF	1.121	EDDM	1.160
7	EDFH	0.189	EDDL	1.105	LFPG	1.157
8	LIRA	0.184	LFPG	1.091	EDDF	1.134
9	LEGE	0.176	LOWW	1.066	EDDL	1.128
10	LEPA	0.166	LIMC	0.968	LSZH	1.017

In Table 2, we list the airports with the largest MNCs for small, intermediate, and large values of ω for eigenvector supracentrality. As expected, for large and small ω , the top airports correspond to the top (i.e., largest eigenvector centrality) airports associated with the aggregation of layers and the Ryanair network layer, respectively. The top-ranked airports for $\omega = 1$ have a large overlap with those for $\omega = 100$; however, the top airport, Adolfo Suárez Madrid–Barajas Airport (LEMD), is particularly interesting. LEMD is the only airport that ranks in the top 10 for both the Ryanair layer and the layer-aggregated network; this contributes to its having the highest rank for this moderate value of ω . We highlight similar ranking boosts for other airports with solid black curves in Fig. 4(b). We also note that LEMD was identified in previous investigations [48, 110] as one of the most important airports in this data set.

In Fig. 5, we illustrate that the eigenvector supracentralities correlate strongly with node degrees. In Fig. 5(a), we show for $\omega = 100$ that the airports’ conditional centralities, averaged across layers, are correlated strongly with their total (i.e., layer-aggregated) degrees $\bar{d}_i = \sum_{t,j} A_{ij}^{(t)}$ (see the blue ‘×’ marks). We expect this strong correlation for eigenvector supracentrality, as node degree is a first-order approximation of eigenvector centrality in monolayer networks [106]. We also plot the mean conditional centralities versus the number of length-2 paths that emanate from each node (see the red circles). As expected, this correlation is even stronger, as the number $\sum_{t,j} [A_{ij}^{(t)}]^2$ of length-2 paths is a second-order approximation to eigenvector centrality [106]³.

³As described in [106], one can interpret the number of length- k paths as an order- k approximation to the dominant eigenvector of \mathbf{A} . Consider the power-method iteration for numerically computing the dominant eigenvector for any matrix \mathbf{B} for which the largest eigenvalue is simply and has magnitude larger than all other eigenvalues. If one initializes the power method with a vector of ones ($\mathbf{1}$), then $\mathbf{B}^k \mathbf{1}$ converges (after normalization) to the dominant eigenvector of the matrix \mathbf{B} . If the matrix happens to be an adjacency matrix, $\mathbf{B} = \mathbf{A}$, then $[\mathbf{A}^k \mathbf{1}]_i$ (i.e., the i th entry of the vector) is equal to the number of length- k paths that emanate from node i .

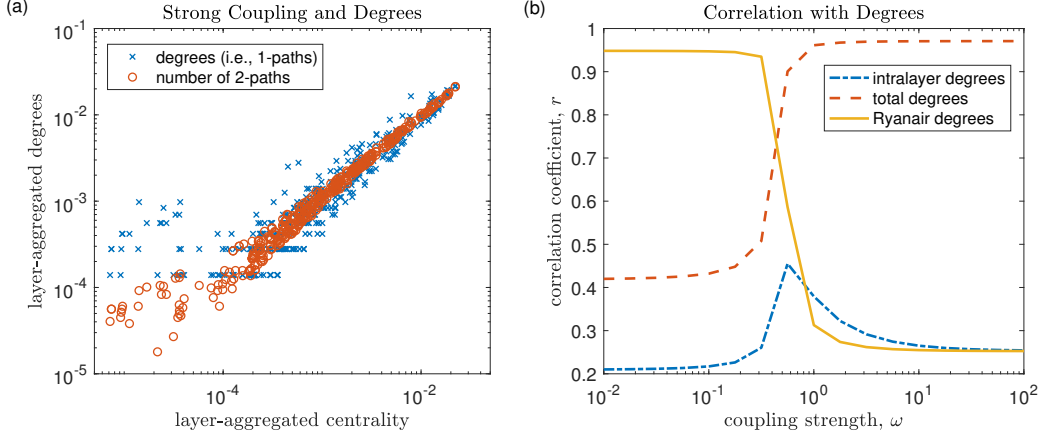


Figure 5. Eigenvector supracentralities for the multiplex European airline network. (a) For $\omega = 100$, the airports’ marginal-node centralities correlate strongly with the layer-aggregated degrees $d_i = \sum_{t,j} A_{ij}^{(t)}$ and with the total number of length-2 paths (summed across layers) that emanating from each node. (To facilitate this comparison, we encode values in normalized vectors.) (b) Pearson correlation coefficients for comparing the airports’ supracentralities to different types of node degree for multiplex networks (see the text).

In Fig. 5(b), we plot (as a function of ω) the Pearson correlation coefficient r between node degrees and eigenvector centralities for three cases: total degrees $\{\bar{d}_i\}$ and marginal node centralities; intralayer degrees $\{d_i^{(t)} = \sum_j A_{ij}^{(t)}\}$ and conditional centralities; and degrees in the Ryanair layer $\{d_i^{(2)} = \sum_j A_{ij}^{(2)}\}$ and marginal node centralities. As expected for very small and large values of ω , the supracentralities correlate strongly with the Ryanair layer and the layer-aggregated network, respectively. Interestingly, for moderate values of ω , there is a spike in the correlation between conditional node centralities and the intralayer degrees $\{d_i^{(t)}\}$.

In Sec. SM2 of the Supplementary Material, we describe the results that we obtain when repeating these computations with PageRank matrices (see Definition 2.5). Figure SM3 is an interesting contrast to Fig. 5(b). Because PageRank matrices have the same spectral radius, no layer dominates in the limit of small ω , so there is no eigenvector localization (see Thm. 4.2). Instead, in Fig. SM3(b), we observe for small ω that the conditional centralities correlate strongly with the nodes’ intralayer degrees $\{d_i^{(t)}\}$.

5.2. United States Mathematical-Science Program Rankings using a Ph.D. Exchange Network [105]. We apply our supracentrality framework to study the prestige of U.S. mathematical-science doctoral-granting programs by examining a temporal network that encodes the graduation and hiring of Ph.D. recipients in the mathematical sciences [105]. We construct the data set using the Mathematics Genealogy Project [85]. As in [105], we calculate uniformly and diagonally coupled authority scores, such that a university with a high authority score corresponds to an academic authority. A high-authority university produces desirable students to be hired by other institutions.

In our study of the Ph.D. exchange network in [105], we restricted our attention to undirected, adjacent-in-time coupling encoded by an interlayer-adjacency matrix $\tilde{\mathbf{A}}$ with entries $\tilde{A}_{tt'} = 1$ if $|t - t'| = 1$ and $\tilde{A}_{tt'} = 0$ otherwise. In the current study, by contrast, we consider the effects of causality by coupling time layers using a directed chain with “layer teleportation” encoded by an interlayer-adjacency matrix with elements

$$(5.1) \quad \tilde{A}_{tt'} = \begin{cases} 1, & t' - t = 1, \\ \gamma, & \text{otherwise.} \end{cases}$$

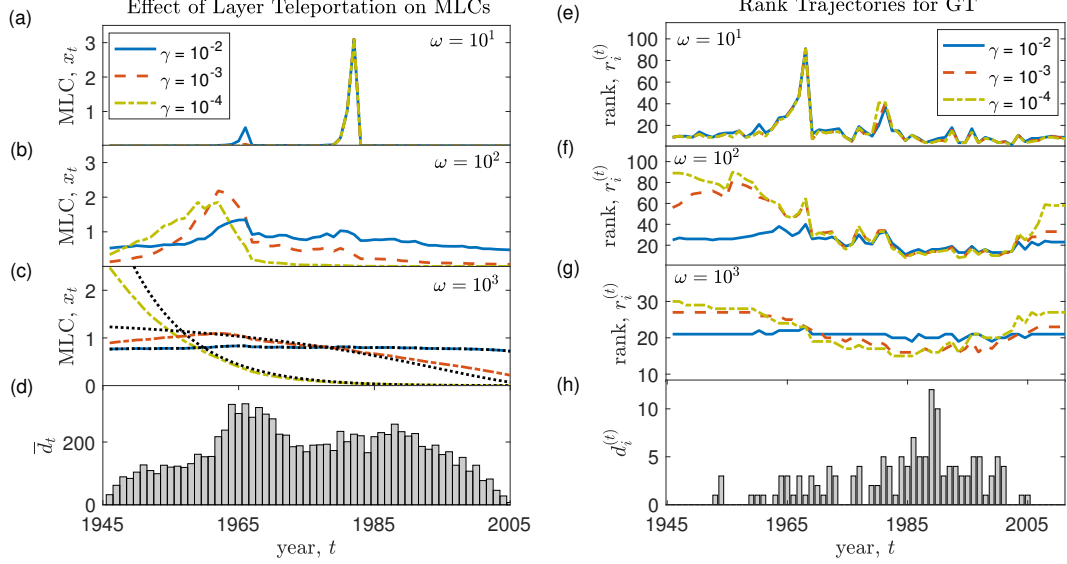


Figure 6. Effect of layer teleportation parameter γ on authority supracentralities in the mathematical-sciences Ph.D. exchange network. (a)–(c) MLC versus year t for several choices of γ and ω . The black dotted curves in panel (c) depict the asymptotic results given by Thm. 4.8: specifically, in the limit $\omega \rightarrow \infty$, the MLC are given by the dominant right eigenvector of $\tilde{\mathbf{A}}$. (d) The total number $\bar{d}_t = \sum_{ij} A_{ij}^{(t)}$ of mathematical-sciences Ph.D. recipients in year t who later supervised a graduating Ph.D. student. (e)–(g) Rank $r_i^{(t)}$ associated with conditional centrality for Georgia Institute of Technology (GT) for various values of γ and ω . (h) The number $d_i^{(t)} = \sum_j A_{ij}^{(t)}$ of people who received a Ph.D. in the mathematical sciences from GT in year t who later supervised a graduating Ph.D. student.

Teleportation was introduced for PageRank centrality [33] to allow the centrality matrices associated with weakly-connected (and even disconnected) networks to satisfy the irreducibility assumptions of Theorems 2.6 and 2.7. Similarly, we use teleportation between layers to satisfy the assumptions of Thm. 3.5; this ensures that the supracentralities are positive and unique. We differentiate these two types of teleportation by referring to the original PageRank notion as *node teleportation* and the teleportation in Eq. 5.1 as *layer teleportation*.

In Fig. 6, we examine the effect of the node teleportation parameter γ on PageRank supracentralities. In Figs. 6(a)–(c), we plot the layers’ authority MLCs $x_t(\omega)$ given by Definition 3.3 versus the year t for three coupling strengths, $\omega \in \{10^1, 10^2, 10^3\}$, which correspond to the weak, intermediate, and strong-coupling regimes. See Sec. 3.3 for a description for how we identify coupling regimes. In each panel, we plot the MLC for three values of the node teleportation parameter: $\gamma = 10^{-2}$, $\gamma = 10^{-3}$, and $\gamma = 10^{-4}$. In panel (d), we plot $\bar{d}_t = \sum_{ij} A_{ij}^{(t)}$, which is the total number of people who received a Ph.D. in the mathematical sciences in year t who later supervised a graduating Ph.D. student. Observe that $t = 1966$ is the year for which \bar{d}_t is the largest.

In Fig. 6(a) (i.e., for small ω), we observe eigenvector localization onto time layer $t = 1982$, whose associated authority matrix has the largest spectral radius among all layers. For $\gamma = 10^{-2}$, we also observe a smaller peak at $t = 1966$, which occurs for moderate values of γ and ω but ultimately vanishes as $\omega \rightarrow 0^+$. Comparing panel (b) to panel (a) for $\gamma = 10^{-2}$, we observe that the peak near $t = 1966$ is more pronounced for $\omega = 10^1$ than for $\omega = 10^2$. We observed a similar localization phenomenon in [105] for adjacent-in-time coupling. In Fig. 6(c), we illustrate behavior that contrasts

starkly with our findings in [105]. Specifically, we see that the interlayer-coupling architecture (which changes with the teleportation parameter γ) has a strong effect on the strong-coupling limit. By varying γ , one can tune the extent to which older time layers have larger centrality than newer time layers. When $\gamma = 10^{-4}$, for example, one can observe in Fig. 6(c) that the MLC of time layers appears to decrease rapidly as t increases. Our asymptotic theory in Sec. 4.2 gives an accurate description of this phenomenon. Observe the dotted black curves, which show the right dominant eigenvector vector $\tilde{\mathbf{v}}^{(1)}$ of $\tilde{\mathbf{A}}$; we obtain these curves from Thm. 4.8 as the asymptotic $\omega \rightarrow \infty$ limit for MLC.

In Figs. 6(e)–(g), we plot the university rank $r_i^{(t)} \in \{1, \dots, N\}$ of Georgia Institute of Technology (GT) associated with its conditional centralities for different time layers; we call this its “rank trajectory”. Similar to panels (a)–(c), these panels depict results for $\omega \in \{10, 10^2, 10^3\}$; in each panel, we again plot results for $\gamma \in \{10^{-2}, 10^{-3}, 10^{-4}\}$. In Fig. 6(h), we plot the number of people who received a Ph.D. in the mathematical sciences from GT who later supervised a graduating Ph.D. student; observe that this increases starting in the 1960s. We used GT in [105] as a case study to illustrate the methods that we developed in that paper. In the current case study, we highlight that the choices for ω and γ influence the centrality trajectory for GT. Note that γ has a larger effect for the intermediate-coupling and strong-coupling regimes (see panels (f) and (g)) than for the weak-coupling regime. Additionally, observe for moderate values of γ and ω that the rank of GT varies from about 50th to about 15th during the period $t \in \{1945, \dots, 1985\}$. In Section SM3 of the Supplementary Materials, we show that although γ has a strong effect on the MLCs for large ω , it does not seem to have a significant effect on top-ranking schools. In Fig. SM4 of the Supplementary Materials, we show that — similar to the results in Fig. 5(b) — for the limit of small and large ω , the authority supracentralities correlate with the intralayer degrees of a dominating layer ($t = 1966$ in this case) and with the nodes’ total degrees, respectively. Note that all centrality trajectories for GT that we present in the present paper differ significantly from those in [105], which implemented coupled time layers using an undirected chain (i.e., adjacent-in-time coupling with undirected interlayer edges between corresponding universities). In particular, many of the rank trajectories in Figs. 6(e)–(g) suggest that GT has its highest rank in the 1980s, around the time when GT graduated its largest numbers of Ph.D. students who subsequently supervised their own Ph.D. students.

6. Conclusions. It is important to develop systematic ways of calculating importances in the form of centrality and its generalizations for nodes, edges, and other structures in multilayer networks. In this paper, we examined centralities based on eigenvectors for two popular classes of multilayer networks: (1) multiplex networks, which encode different types of relationships; and (2) temporal networks, in which the relationships change in time. We presented a unifying linear-algebraic framework that generalizes eigenvector-based centralities, such as PageRank and hub/authority scores, for multiplex and temporal networks. A key aspect of our approach involves studying joint, marginal, and conditional centralities that one calculates from the dominant eigenvector of a supracentrality matrix, which couples centrality matrices that are associated with individual layers. See [102] for MATLAB code that computes supracentralities and reproduces the experimental results of the present paper.

Our main methodological contribution is the extension of the supracentrality framework of [105], which previously was restricted to undirected adjacent-in-time coupling, to more general types of interlayer coupling. Our new, more general framework couples layers through an interlayer-adjacency matrix $\tilde{\mathbf{A}}$, allowing one to study centralities in multilayer networks with a large family of interlayer coupling topologies. We found that $\tilde{\mathbf{A}}$ significantly impacts supracentralities, and we highlighted that some choices are more appropriate than others for different applications. As an example, in Sec. 5.2, we let $\tilde{\mathbf{A}}$ encode a directed chain with layer teleportation (see Fig. 1(b) for a visualization) and studied a temporal network that encodes the graduation and hiring of Ph.D. recipients in the mathematical sciences. Our results contrast sharply with those in [105] because of our different choice of interlayer coupling. In the present paper, one of our observations is that coupling layers using a directed chain (which respects the arrow of time) introduces a bias that increases the centralities of node-layer pairs

associated with the earliest time layers. Additionally, we illustrated that one can moderate such a bias using a layer teleportation parameter (and it seems fruitful to study multilayer generalizations of so-called “smart teleportation” [59] in the future). We also studied a multiplex network that encodes airline transportation in Europe (see Sec. 5.1), where another mechanism yielded boosts in centrality. Specifically, we observed that nodes that are important in both the large- ω and small- ω limits can receive centrality boosts for moderate ω over nodes that are important in just one of the limits. For one illustration, see the centrality of the airport LEMB in Table 2 and the black curves in Fig. 4(b).

We explored how different interlayer-coupling architectures (as encoded by $\tilde{\mathbf{A}}$) and interlayer-coupling strengths (as encoded by ω) influence centralities. Specifically, we identified an interesting interplay between $\tilde{\mathbf{A}}$ and the architectures of the individual layers in multiplex and temporal networks. To gain insight into this interplay, we constructed a singular perturbation theory for the limits of weak and strong interlayer coupling (see Sec. 4), which lead to layer decoupling and layer aggregation, respectively. We demonstrated that the limiting supracentralities depend on several factors, including the dominant left and right eigenvectors of $\tilde{\mathbf{A}}$ and the spectral radii of the layers’ centrality matrices, possibly leading to localization of the dominant eigenvector of a supracentrality matrix onto one or more layers (specifically, the ones whose associated centrality matrices have the largest spectral radii).

We expect that our results will be useful not only for centrality analysis, but also for other matrices that arise in the course of data integration. In the context of our problem, we considered both (i) a set of matrices and (ii) a set of relationships between these matrices. Using a “supramatrix” framework, we constructed and analyzed a matrix that reflects both (i) and (ii). Our perturbative approach for analyzing dominant eigenspaces in the present paper assumes that the matrices are nonnegative and square, but it is not limited to matrices that encode network data. Consequently, we expect our findings to also be insightful in other scenarios that involve combining matrices of data into larger matrices.

Appendix A. Proof of Theorem 3.5.

To prove the uniqueness and positivity of $\mathfrak{v}(\omega)$, we use the Perron–Frobenius theorem for nonnegative matrices (see Thm. 2.6) [4]. To satisfy the assumptions of Thm. 2.6, we must show that the matrix $\mathbb{C}(\omega)$ is nonnegative and irreducible under our two assumptions: (i) $\tilde{\mathbf{A}}$ is nonnegative and irreducible; and (ii) the sum $\sum_t \mathbf{C}^{(t)}$ is an irreducible nonnegative matrix. By construction, the entries in $\mathbb{C}(\omega)$ are nonnegative, so we only need to prove irreducibility. Because the matrix $\mathbb{C}(\omega)$ is nonnegative, we can interpret it as a weighted adjacency matrix that encodes (possibly) directed and weighted edges between node-layer pairs $\{(i, t)\}$ for $i \in \mathcal{V} = \{1, \dots, N\}$ and $t \in \{1, \dots, T\}$. We will show that the network associated with the adjacency matrix $\mathbb{C}(\omega)$ is strongly connected, which implies irreducibility.

We start with two observations. First, we note $\tilde{\mathbf{A}}$ describes an adjacency matrix for a strongly connected network, and we let $\tilde{L} < \infty$ denote its diameter. For any node k and any two layers t and t' , it follows that there exists a path in the network associated with the adjacency matrix $\mathbb{C}(\omega)$ from node-layer pair (k, t) to node-layer pair (k, t') . The length of this path is at most \tilde{L} . Second, because the matrix $\overline{\mathbf{C}}^{(t)} = T^{-1} \sum_t \mathbf{C}^{(t)}$ is irreducible and nonnegative, we can interpret it as an adjacency matrix for a strongly connected network. Let $L < \infty$ denote its diameter. For any two nodes i and j of this network, it follows that there exists a path of length $l \leq L$ from i to j . We denote the path by a sequence $\mathcal{P}(i, j) = \{k_0, k_1, \dots, k_{l-1}, k_l\}$ of nodes from $i = k_0$ to $j = k_l$. We also identify a sequence $\{t_1, t_2, \dots, t_l\}$ of layers, such that the entry $[\mathbf{C}^{(t_j)}]_{k_{j-1}, k_j}$ in matrix $\mathbf{C}^{(t_j)}$ is positive. For any j , there must exist at least one matrix $\mathbf{C}^{(t_j)}$ for which the (k_{j-1}, k_j) -th entry is positive, because the (k_{j-1}, k_j) -th entry in $\overline{\mathbf{C}}^{(t)}$ is positive (i.e., because (k_{j-1}, k_j) is an edge), and $\overline{\mathbf{C}}^{(t)}$ is a sum of nonnegative matrices.

For any two node-layer pairs (i, s) and (j, t) , we now prove that there exists a path, of length at most $\tilde{L}L$, from (i, s) to (j, t) in the network associated with the matrix $\mathbb{C}(\omega)$. We do this by explicitly constructing such a path. We first identify a path $\mathcal{P}(i, j)$ from i to j in the network associated with

$\overline{\mathbf{C}^{(t)}}$. Consider the following sequence of node-layer pairs:

$$(A.1) \quad \{(k_0, t_0), (k_1, t_1), (k_2, t_2), \dots, (k_{l-1}, t_{l-1}), (k_l, t_l)\},$$

where $l \leq L$; we define k_j and t_j as above; and we take $k_0 = i$, $t_0 = s$, $k_l = j$, and $t_l = t$. By definition, the (k_{j-1}, k_j) -th entry in $\mathbf{C}^{(t_j)}$ is positive for each j , implying that the network associated with matrix $\mathbf{C}(\omega)$ has an edge from (k_{j-1}, t_j) to (k_j, t_j) . We construct a path from (i, s) to (j, t) by taking the sequence given by Eq. (A.1) and inserting a path from each term in the sequence to the next term. That is, we insert a path from (k_0, t_0) to (k_0, t_1) using only node-layer pairs that involve node k_0 . The length of the path is at most \tilde{L} . Additionally, from our definition of the path $P(i, j)$, we see that there exists an edge from (k_0, t_1) to (k_1, t_1) . We then insert a path, whose length is also at most \tilde{L} , from (k_1, t_1) to (k_1, t_2) using only node-layer pairs that involve node k_1 . There also exists an edge from (k_1, t_2) to (k_2, t_2) , and so on. We repeat this process until finally we insert a path from (k_{l-1}, t_{l-1}) to (k_{l-1}, t_l) using only node-layer pairs that involve node k_{l-1} , and we note that there exists an edge from (k_{l-1}, t_l) to (k_l, t_l) . Each of these paths exists because the network associated with $\hat{\mathbf{A}}$ is strongly connected, and each of these paths has a length of at most \tilde{L} .

This construction yields a path from any node-layer pair to any other node-layer pair in the network associated with $\mathbf{C}(\omega)$, which proves that the network is strongly connected. We have also obtained an upper bound on the diameter, which is at most $\tilde{L}L$. Because $\mathbf{C}(\omega)$ corresponds to a strongly connected network, it is irreducible and nonnegative due to the Perron–Frobenius theorem for nonnegative matrices, and so the dominant right eigenvector $\mathbf{v}(\omega)$ is unique and positive. Consequently, the entries $\{W_{it}(\omega)\}$, $\{x_i(\omega)\}$, and $\{\hat{x}_i(\omega)\}$ are also unique and positive. Because these entries are positive, it follows in turn that $\{Z_{it}(\omega)\}$ and $\{\hat{Z}_{it}(\omega)\}$ are positive and finite-valued.

Finally, if $\mathbf{C}(\omega)$ is also aperiodic, then Thm. 2.6 states that the largest positive eigenvalue of $\mathbf{C}(\omega)$ is larger in magnitude than the other eigenvalues.

Appendix B. Proof of Theorem 4.1. For any choice of matrix norm, $\|\mathbf{C}(\omega) - \hat{\mathbf{C}}\| = \omega \|\hat{\mathbf{A}}\| \rightarrow 0^+$ as $\omega \rightarrow 0^+$ (recall that $\hat{\mathbf{A}} = \hat{\mathbf{A}} \otimes \mathbf{I}$), implying that

$$(B.1) \quad \mathbf{C}(\omega) \rightarrow \hat{\mathbf{C}} = \text{diag} \left[\mathbf{C}^{(1)}, \mathbf{C}^{(2)}, \dots, \mathbf{C}^{(T)} \right].$$

We assume that the eigenvalues $\{\mu_i^{(t)}\}$ of each $\mathbf{C}^{(t)}$ are simple and that $\{\mu_i^{(t)}\} \cap \{\mu_i^{(t')}\} = \emptyset$ for $t \neq t'$. We consider the matrix–vector multiplication $\hat{\mathbf{C}}\mathbf{v}^{(i,t)}$, and we use $k = s \bmod(N)$ and $t' = \lceil s/jN \rceil$ to obtain

$$(B.2) \quad [\hat{\mathbf{C}}\mathbf{v}^{(i,t)}]_s = \sum_{(k,t')} C_{jk}^{(t)} v_k^{(i,t')} \delta_{tt'} = \mu_i^{(t)} v_j^{(i,t')} \delta_{tt'} = \mu_i^{(t)} [\mathbf{v}^{(i,t)}]_s.$$

(Recall that we use the notation $[\hat{\mathbf{C}}\mathbf{v}^{(i,t)}]_s$ to denote the s -th entry of the vector $\hat{\mathbf{C}}\mathbf{v}^{(i,t)}$.) This implies that $\hat{\mathbf{C}}\mathbf{v}^{(i,t)} = \mu_i^{(t)} \mathbf{v}^{(i,t)}$, so $\mu_i^{(t)}$ is an eigenvalue of $\hat{\mathbf{C}}$ with right eigenvector $\mathbf{v}^{(i,t)}$. Similarly, $\hat{\mathbf{C}}^T \mathbf{u}^{(i,t)} = \mu_i^{(t)} \mathbf{u}^{(i,t)}$, so $\mathbf{u}^{(i,t)}$ is the associated left eigenvector.

We now show that when the eigenvalue $\mu_i^{(t)}$ is not simple, such that $\mu_i^{(t)} = \lambda_n(0)$ for some set $\mathcal{P} = \{(i, t)\}$ with cardinality $P = |\mathcal{P}| > 1$, it has P -dimensional left and right eigenspaces that are spanned by the associated left and right eigenvectors $\{\mathbf{u}^{(i,t)}\}$ and $\{\mathbf{v}^{(i,t)}\}$. To see this, let $\tilde{\mathbf{u}} = \sum_{(i,t)} \beta_{i,t} \mathbf{u}^{(i,t)}$ and $\tilde{\mathbf{v}} = \sum_{(i,t)} \alpha_{i,t} \mathbf{v}^{(i,t)}$ denote any linear combination of such vectors, and consider the matrix–vector

multiplication

$$\begin{aligned}
[\hat{\mathbb{C}}\tilde{\mathbf{v}}]_s &= \sum_{(k,t')} C_{jk}^{(t)} \sum_{(i,t) \in \mathcal{P}} \alpha_{i,t} v_k^{(i,t')} \delta_{tt'} \\
&= \sum_{(i,t) \in \mathcal{P}} \alpha_{i,t} \mu_i^{(t)} v_j^{(i,t)} \delta_{tt'} \\
&= \lambda_n \sum_{(i,t) \in \mathcal{P}} \alpha_{i,t} v_j^{(i,t)} \delta_{tt'} \\
\text{(B.3)} \quad &= \lambda_n [\tilde{\mathbf{v}}]_s,
\end{aligned}$$

so that $\hat{\mathbb{C}}\tilde{\mathbf{v}} = \lambda_n \tilde{\mathbf{v}}$. One shows similarly that $\hat{\mathbb{C}}^T \tilde{\mathbf{u}} = \lambda_n \tilde{\mathbf{u}}$, which completes the proof.

Appendix C. Proof of Theorem 4.2. Equation (4.1) follows directly from Thm. 4.1, so the $\omega \rightarrow 0^+$ limiting dominant eigenvalue $\lambda_{\max}(0)$ has a P -dimensional dominant eigenspace that is spanned by the left and right eigenvectors, $\{\mathbf{u}^{(i,t)}\}$ and $\{\mathbf{v}^{(i,t)}\}$ for $(i,t) \in \mathcal{P} = \{(i,t) : \mu_i^{(t)} = \lambda_{\max}(0)\}$. We still need to prove that the constants $\{\alpha_p\}$ and $\{\beta_p\}$ satisfy Eqs. (4.2).

We expand $\lambda_{\max}(\omega)$, $\mathbf{u}^{(1)}(\omega)$, and $\mathbf{v}^{(1)}(\omega)$ for small ω to obtain order- k approximations:

$$\begin{aligned}
\lambda_{\max}(\omega) &= \sum_{j=0}^k \omega^j \lambda_j + \mathcal{O}(\omega^{k+1}), \\
\mathbf{v}^{(1)}(\omega) &= \sum_{j=0}^k \omega^j \mathbf{v}_j + \mathcal{O}(\omega^{k+1}), \\
\text{(C.1)} \quad \mathbf{u}^{(1)}(\omega) &= \sum_{j=0}^k \omega^j \mathbf{u}_j + \mathcal{O}(\omega^{k+1}).
\end{aligned}$$

We use superscripts to indicate powers of ω in the terms in the expansion, and we use subscripts for the terms that are multiplied by the power of ω . Note that λ_0 , \mathbf{u}_0 , and \mathbf{v}_0 , respectively, indicate the dominant eigenvalue and its corresponding left and right eigenvectors in the limit $\omega \rightarrow 0^+$. Successive terms in these expansions represent higher-order derivatives, and each term assumes appropriate smoothness of these functions.

Our strategy is to develop consistent solutions to both $\mathbb{C}(\omega)^T \mathbf{u}^{(1)}(\omega) = \lambda_{\max}(\omega) \mathbf{u}^{(1)}(\omega)$ and $\mathbb{C}(\omega) \mathbf{v}^{(1)}(\omega) = \lambda_{\max}(\omega) \mathbf{v}^{(1)}(\omega)$ for progressively larger values of k . Starting with the first-order approximation, we insert $\lambda_{\max}(\omega) \approx \lambda_0 + \omega \lambda_1$ and $\mathbf{v}^{(1)}(\omega) \approx \mathbf{v}_0 + \omega \mathbf{v}_1$ into Eq. (3.2) and collect the zeroth-order and first-order terms in ω to obtain

$$\text{(C.2)} \quad (\lambda_0 \mathbb{I} - \hat{\mathbb{C}}) \mathbf{v}_0 = 0,$$

$$\text{(C.3)} \quad (\lambda_0 \mathbb{I} - \hat{\mathbb{C}}) \mathbf{v}_1 = (\hat{\mathbb{A}} - \lambda_1 \mathbb{I}) \mathbf{v}_0,$$

where \mathbb{I} is the $NT \times NT$ identity matrix. Equation (C.2) corresponds to the system described by Thm. 4.1, implying that the operator $\lambda_0 \mathbb{I} - \hat{\mathbb{C}}$ is singular and has a K -dimensional null space, where $K = |\{t : \mu_t = \max_t \mu_t\}|$ is the number of centrality matrices $\mathbf{C}^{(t)}$ whose largest eigenvalue is equal to the maximum eigenvalue. In particular, $\max_t \mu_t = \lambda_0 = \lambda_{\max}(0)$, and the dominant eigenvectors have the general form

$$\text{(C.4)} \quad \mathbf{v}_0 = \sum_t \alpha_t \mathbf{v}^{(1,t)}, \quad \mathbf{u}_0 = \sum_t \beta_t \mathbf{u}^{(1,t)},$$

where $\{\alpha_t\}$ and $\{\beta_t\}$ are constants that satisfy $1 = \sum_t \alpha_t^2 = \sum_t \beta_t^2$ to ensure that $\|\alpha\| = \|\beta\| = 1$. (See Thm. 4.1 for definitions of $\mathbf{u}^{(1,t)}$ and $\mathbf{v}^{(1,t)}$.)

To determine the vectors $\alpha = [\alpha_1, \dots, \alpha_T]^T$ and $\beta = [\beta_1, \dots, \beta_T]^T$ of constants that uniquely determine \mathbf{u}_0 and \mathbf{v}_0 , we use Eq. (C.3) to seek a solvability condition for the first-order terms. We use the fact that the left null space of $\lambda_0 \mathbb{I} - \tilde{\mathbf{C}}$ is the span of $\{\mathbf{u}^{(1,t)}\}$ to see that $[\mathbf{u}^{(1,t)}]^T (\lambda_0 \mathbb{I} - \tilde{\mathbf{C}}) \mathbf{v}_1 = 0$ for any t . We left-multiply Eq. (C.3) by $[\mathbf{u}^{(1,t)}]^T$ and simplify to obtain

$$(C.5) \quad [\mathbf{u}^{(1,t)}]^T \hat{\mathbf{A}} \mathbf{v}_0 = \lambda_1 [\mathbf{u}^{(1,t)}]^T \mathbf{v}_0.$$

Using the solution of \mathbf{v}_0 given by Eq. (C.4), we obtain

$$(C.6) \quad \begin{aligned} \sum_{t'} \alpha_{t'} [\mathbf{u}^{(1,t)}]^T \hat{\mathbf{A}} \mathbf{v}^{(1,t')} &= \lambda_1 \sum_{t'} \alpha_{t'} [\mathbf{u}^{(1,t)}]^T \mathbf{v}^{(1,t')} \\ &= \lambda_1 \langle \mathbf{u}^{(1,t)}, \mathbf{v}^{(1,t)} \rangle \alpha_t, \end{aligned}$$

which uses $[\mathbf{u}^{(1,t)}]^T \mathbf{v}^{(1,t)} = \langle \mathbf{u}^{(1,t)}, \mathbf{v}^{(1,t')} \rangle \delta_{tt'}$, where δ_{ij} is the Kronecker delta. We simplify the left-hand-side of Eq. (C.6) to obtain

$$(C.7) \quad \begin{aligned} \sum_{t'} \alpha_{t'} [\mathbf{u}^{(1,t)}]^T \hat{\mathbf{A}} \mathbf{v}^{(1,t')} &= \sum_{t'} \alpha_{t'} A_{t,t'} [\mathbf{u}^{(1,t)}]^T [\mathbf{e}^{(t')} \otimes \mathbf{v}^{(1,t')}] \\ &= \sum_{t'} \alpha_{t'} A_{t,t'} [\mathbf{e}^{(t)} \otimes \mathbf{u}^{(1,t)}]^T [\mathbf{e}^{(t')} \otimes \mathbf{v}^{(1,t')}] \\ &= \sum_{t'} \alpha_{t'} A_{t,t'} \langle \mathbf{u}^{(1,t)}, \mathbf{v}^{(1,t')} \rangle. \end{aligned}$$

The last expression follows from the relations $\hat{\mathbf{A}} = \tilde{\mathbf{A}} \otimes \mathbf{I}$, $\mathbf{v}^{(1,t')} = \mathbf{e}^{(t')} \otimes \mathbf{v}^{(1,t')}$, and $\mathbf{u}^{(1,t)} = \mathbf{e}^{(t)} \otimes \mathbf{u}^{(1,t)}$, where we recall that $\mathbf{e}^{(t)}$ is a unit vector that consists of 0s except for entry t , which is a 1. We set Eq. (C.7) equal to Eq. (C.6) and divide by $\langle \mathbf{u}^{(1,t)}, \mathbf{v}^{(1,t)} \rangle$ to obtain the dominant right eigenvalue equation

$$(C.8) \quad \sum_{t'} A_{t,t'} \frac{\langle \mathbf{u}^{(1,t)}, \mathbf{v}^{(1,t')} \rangle}{\langle \mathbf{u}^{(1,t)}, \mathbf{v}^{(1,t)} \rangle} \alpha_{t'} = \lambda_1 \alpha_t.$$

One proceeds analogously to obtain the left dominant eigenvector equations, and together these two eigenvector equations yield Eq. (4.2).

Appendix D. Proof of Theorem 4.7. Examining $\tilde{\mathbf{C}}(\epsilon)$, which is given by Eq. (4.7), yields (using any matrix norm) $\|\tilde{\mathbf{C}}(\epsilon) - \hat{\mathbf{A}}\| = \epsilon \|\tilde{\mathbf{C}}\| \rightarrow 0^+$ as $\epsilon \rightarrow 0^+$, implying that $\tilde{\mathbf{C}}(0) = \hat{\mathbf{A}} = \tilde{\mathbf{A}} \otimes \mathbf{I}$. Using the stride permutation \mathbb{P} defined by Eq. (4.8), we can write

$$(D.1) \quad \mathbb{P}^T (\tilde{\mathbf{A}} \otimes \mathbf{I}) \mathbb{P} = \mathbf{I} \otimes \tilde{\mathbf{A}} = \begin{bmatrix} \tilde{\mathbf{A}} & 0 & \cdots \\ 0 & \tilde{\mathbf{A}} & \ddots \\ \vdots & \ddots & \ddots \end{bmatrix}.$$

Because $\mathbf{I} \otimes \tilde{\mathbf{A}}$ is block diagonal and each diagonal block is identical, it follows that the spectrum of $\mathbf{I} \otimes \tilde{\mathbf{A}}$ is identical to that of $\tilde{\mathbf{A}}$ (although the eigenvalues need to repeat an appropriate number of times), and one can obtain the eigenvectors of the former as functions of the eigenvectors of $\tilde{\mathbf{A}}$, which we assume to be diagonalizable.

Let $\{\tilde{\mu}_t\}$ denote the eigenvalues of $\tilde{\mathbf{A}}$, and let $\tilde{\mathbf{u}}^{(t)}$ and $\tilde{\mathbf{v}}^{(t)}$ denote the corresponding left and right eigenvectors, respectively. We now illustrate that $\tilde{\mathbf{u}}^{(t,j)} = \tilde{\mathbf{e}}^{(j)} \otimes \mathbf{u}^{(t)}$ and $\tilde{\mathbf{v}}^{(t,j)} = \tilde{\mathbf{e}}^{(j)} \otimes \mathbf{v}^{(t)}$ are left and right eigenvectors of $\mathbf{I} \otimes \tilde{\mathbf{A}}$. With $s \in \{1, \dots, TN\}$, we define $t = s \bmod(T)$ and $k = \lceil t/sT \rceil$ and obtain

$$\begin{aligned}
[(\mathbf{I} \otimes \tilde{\mathbf{A}})\tilde{\mathbf{v}}^{(t,j)}]_s &= \sum_{t',k'} \tilde{A}_{tt'} \delta_{kk'} \tilde{v}_{t'}^{(t)} \delta_{k'j} \\
&= \sum_{t',k'} \tilde{A}_{tt'} \tilde{v}_{t'}^{(t)} \delta_{kj} \\
&= \sum_{t'} \tilde{A}_{tt'} \tilde{v}_{t'}^{(t)} \delta_{kj} \\
&= \tilde{\mu}_t \tilde{v}_{t'}^{(t)} \delta_{kj} \\
\text{(D.2)} \qquad \qquad \qquad &= \tilde{\mu}_t [\tilde{\mathbf{v}}^{(t,j)}]_s.
\end{aligned}$$

One can show similarly that $(\mathbf{I} \otimes \tilde{\mathbf{A}})^T \tilde{\mathbf{u}}^{(t,j)} = \tilde{\mu}_t \tilde{\mathbf{u}}^{(t,j)}$, illustrating that $\tilde{\mathbf{u}}^{(t,j)}$ and $\tilde{\mathbf{v}}^{(t,j)}$ are left and right eigenvectors associated to each eigenvalue $\tilde{\mu}_t$ of $\mathbf{I} \otimes \tilde{\mathbf{A}}$. This implies that $\mathbb{P}^T(\tilde{\mathbf{A}} \otimes \mathbf{I})\mathbb{P}\tilde{\mathbf{v}}^{(t,j)} = \mu_t \tilde{\mathbf{v}}^{(t,j)}$, and left-multiplication by \mathbb{P} gives

$$\text{(D.3)} \qquad \qquad \qquad (\tilde{\mathbf{A}} \otimes \mathbf{I})[\mathbb{P}\tilde{\mathbf{v}}^{(t,j)}] = \tilde{\mu}_t [\mathbb{P}\tilde{\mathbf{v}}^{(t,j)}].$$

By repeating this procedure using $(\tilde{\mathbf{A}} \otimes \mathbf{I})^T$ rather than $(\tilde{\mathbf{A}} \otimes \mathbf{I})$, one can also show that $(\tilde{\mathbf{A}} \otimes \mathbf{I})^T [\mathbb{P}\tilde{\mathbf{u}}^{(t,j)}] = \tilde{\mu}_t [\mathbb{P}\tilde{\mathbf{u}}^{(t,j)}]$. Taken together, these two expressions imply that $\mathbb{P}\tilde{\mathbf{u}}^{(t,j)}$ and $\mathbb{P}\tilde{\mathbf{v}}^{(t,j)}$ are left and right eigenvectors of $\hat{\mathbf{A}} = \tilde{\mathbf{A}} \otimes \mathbf{I}$ associated with the eigenvalue $\tilde{\mu}_t$. However, for a given value of t (and assuming that the eigenvalues $\{\tilde{\mu}_t\}$ are simple), there are N orthogonal left eigenvectors $\{\mathbb{P}\tilde{\mathbf{u}}^{(t,j)}\}$ and N orthogonal right eigenvectors $\{\mathbb{P}\tilde{\mathbf{v}}^{(t,j)}\}$ for $j \in \{1, \dots, N\}$. It follows that each eigenvalue $\tilde{\mu}_t$ of $\hat{\mathbf{A}}$ has multiplicity N and N -dimensional left and right eigenspaces.

Appendix E. Proof of Theorem 4.8. We expand $\tilde{\lambda}_{\max}(\epsilon)$, $\tilde{\mathbf{v}}^{(1)}(\epsilon)$, and $\tilde{\mathbf{u}}^{(1)}(\epsilon)$ for small ϵ to obtain order- k approximations:

$$\begin{aligned}
\tilde{\lambda}_{\max}(\epsilon) &= \sum_{j=0}^k \epsilon^j \tilde{\lambda}_j + \mathcal{O}(\epsilon^{k+1}), \\
\tilde{\mathbf{v}}^{(1)}(\epsilon) &= \sum_{j=0}^k \epsilon^j \tilde{\mathbf{v}}_j + \mathcal{O}(\epsilon^{k+1}), \\
\tilde{\mathbf{u}}^{(1)}(\epsilon) &= \sum_{j=0}^k \epsilon^j \tilde{\mathbf{u}}_j + \mathcal{O}(\epsilon^{k+1}).
\end{aligned}
\text{(E.1)}$$

We use superscripts to indicate powers of ϵ in the terms in the expansion and subscripts for the terms that are multiplied by ϵ^j . Note that $\tilde{\lambda}_0$, $\tilde{\mathbf{v}}_0$, and $\tilde{\mathbf{u}}_0$, respectively, indicate the dominant eigenvalue and corresponding right and left eigenvectors in the limit $\epsilon \rightarrow 0^+$. Successive terms in these expansions represent higher-order derivatives, and each term assumes appropriate smoothness of these functions.

Our strategy is to develop consistent solutions to $\tilde{\mathbf{C}}(\epsilon)^T \tilde{\mathbf{u}}(\epsilon) = \tilde{\lambda}_{\max}(\epsilon) \tilde{\mathbf{u}}(\epsilon)$ and $\tilde{\mathbf{C}}(\epsilon) \tilde{\mathbf{v}}(\epsilon) = \tilde{\lambda}_{\max}(\epsilon) \tilde{\mathbf{v}}(\epsilon)$ for progressively larger values of k . Starting with the first-order approximation, we insert $\tilde{\lambda}_{\max}(\epsilon) \approx \tilde{\lambda}_0 + \epsilon \tilde{\lambda}_1$ and $\tilde{\mathbf{v}}(\epsilon) \approx \tilde{\mathbf{v}}_0 + \epsilon \tilde{\mathbf{v}}_1$ into Eq. (3.2) and collect the zeroth-order and first-order terms in ϵ to obtain

$$\text{(E.2)} \qquad \qquad \qquad (\tilde{\lambda}_0 \mathbf{I} - \hat{\mathbf{A}}) \tilde{\mathbf{v}}_0 = 0,$$

$$\text{(E.3)} \qquad \qquad \qquad (\tilde{\lambda}_0 \mathbf{I} - \hat{\mathbf{A}}) \tilde{\mathbf{v}}_1 = (\hat{\mathbf{C}} - \tilde{\lambda}_1 \mathbf{I}) \tilde{\mathbf{v}}_0,$$

where \mathbb{I} is the $NT \times NT$ identity matrix. Equation (E.2) corresponds to the system described by Thm. 4.1, implying that the operator $\tilde{\lambda}_0 \mathbb{I} - \hat{\mathbb{A}}$ is singular and has an N -dimensional null space. (This is the dominant eigenspace of $\hat{\mathbb{A}}$.) Specifically, Eq. (E.2) has a general solution of the form

$$(E.4) \quad \begin{aligned} \tilde{\mathbf{w}}_0 &= \sum_j \tilde{\alpha}_j \mathbb{P} \tilde{\mathbf{v}}^{(1,j)}, \\ \tilde{\lambda}_0 &= \max_t \tilde{\mu}_t, \end{aligned}$$

where $\{\tilde{\alpha}_i\}$ are constants that satisfy $\sum_i \tilde{\alpha}_i^2 = 1$ (so that $\|\tilde{\mathbf{w}}_0\|_2 = 1$). Additionally,

$$(E.5) \quad \tilde{\mathbf{u}}_0 = \sum_j \tilde{\beta}_j \mathbb{P} \tilde{\mathbf{u}}^{(1,j)},$$

where $\sum_i \tilde{\beta}_i^2 = 1$ (so that $\|\tilde{\mathbf{u}}_0\|_2 = 1$).

To determine the vectors $\tilde{\boldsymbol{\alpha}} = [\tilde{\alpha}_1, \dots, \tilde{\alpha}_N]^T$ and $\tilde{\boldsymbol{\beta}} = [\tilde{\beta}_1, \dots, \tilde{\beta}_N]^T$ of constants that uniquely determine $\tilde{\mathbf{u}}_0$ and $\tilde{\mathbf{w}}_0$, we seek a solvability condition for the first-order terms. Using the fact that the left null space of $\tilde{\lambda}_0 \mathbb{I} - \hat{\mathbb{A}}$ is the span of $\{\mathbb{P} \tilde{\mathbf{u}}^{(1,i)}\}$, it follows that $[\tilde{\mathbf{u}}^{(1,i)}]^T \mathbb{P}^T (\tilde{\lambda}_0 \mathbb{I} - \hat{\mathbb{A}}) \tilde{\mathbf{w}}_0 = 0$. Therefore, we left-multiply Eq. (E.3) by $[\tilde{\mathbf{u}}^{(1,i)}]^T \mathbb{P}^T$ and simplify to obtain

$$(E.6) \quad [\tilde{\mathbf{u}}^{(1,i)}]^T \mathbb{P}^T \hat{\mathbb{C}} \tilde{\mathbf{w}}_0 = \tilde{\lambda}_1 [\tilde{\mathbf{u}}^{(1,i)}]^T \mathbb{P}^T \tilde{\mathbf{w}}_0.$$

Using the solution of $\tilde{\mathbf{w}}_0$ in Eq. (E.4), we obtain

$$(E.7) \quad \begin{aligned} \sum_j \tilde{\alpha}_j [\tilde{\mathbf{u}}^{(1,i)}]^T \mathbb{P}^T \hat{\mathbb{C}} \mathbb{P} \tilde{\mathbf{v}}^{(1,j)} &= \tilde{\lambda}_1 \sum_j \tilde{\alpha}_j [\tilde{\mathbf{u}}^{(1,i)}]^T \mathbb{P}^T \mathbb{P} \tilde{\mathbf{v}}^{(1,j)} \\ &= \tilde{\lambda}_1 \sum_j \tilde{\alpha}_j [\tilde{\mathbf{u}}^{(1,i)}]^T \tilde{\mathbf{v}}^{(1,j)} \\ &= \tilde{\lambda}_1 \langle \tilde{\mathbf{u}}^{(1)}, \tilde{\mathbf{v}}^{(1)} \rangle \tilde{\alpha}_i, \end{aligned}$$

because $\mathbb{P}^T \mathbb{P} = \mathbb{P} \mathbb{P}^T = \mathbb{I}$ and $[\tilde{\mathbf{u}}^{(1,i)}]^T \tilde{\mathbf{v}}^{(1,j)} = \langle \tilde{\mathbf{u}}^{(1)}, \tilde{\mathbf{v}}^{(1)} \rangle \delta_{ij}$, where δ_{ij} is the Kronecker delta. We divide by Eq. (E.7) by $\langle \tilde{\mathbf{u}}^{(1)}, \tilde{\mathbf{v}}^{(1)} \rangle$ to obtain an N -dimensional eigenvalue equation for the dominant eigenvector $\tilde{\boldsymbol{\alpha}}$. One can implement the analogous steps for the left dominant eigenvector equations, and together these two eigenvector equations yield Eq. (4.11).

REFERENCES

- [1] W. AHMAD, M. A. PORTER, AND M. BEGUERISSE-DÍAZ, *Tie-decay temporal networks in continuous time and eigenvector-based centralities*, arXiv preprint arXiv:1805.00193, (2018).
- [2] A. ALSAYED AND D. J. HIGHAM, *Betweenness in time dependent networks*, *Chaos, Solitons & Fractals*, 72 (2015), pp. 35–48.
- [3] F. ARRIGO AND D. J. HIGHAM, *Sparse matrix computations for dynamic network centrality*, *Applied Network Science*, 2 (2017), p. 17.
- [4] R. B. BAPAT AND T. E. S. RAGHAVAN, *Nonnegative Matrices and Applications*, vol. 64, Cambridge University Press, 1997.
- [5] M. BARDOSCIA, G. BIANCONI, AND G. FERRARA, *Multiplex network analysis of the UK OTC derivatives market*, (2018). Preprint, available at https://papers.ssrn.com/sol3/papers.cfm?abstract_id=3180709.
- [6] D. S. BASSETT, N. F. WYMBS, M. P. ROMBACH, M. A. PORTER, P. J. MUCHA, AND S. T. GRAFTON, *Task-based core-periphery organization of human brain dynamics*, *PLoS computational biology*, 9 (2013), p. e1003171.

- [7] F. BATTISTON, V. NICOSIA, AND V. LATORA, *Structural measures for multiplex networks*, Physical Review E, 89 (2014), p. 032804.
- [8] G. BIANCONI, *Multilayer Networks: Structure and Function*, Oxford University Press, 2018.
- [9] S. BOCCALETTI, G. BIANCONI, R. CRIADO, C.I. DEL GENIO, J. GÓMEZ-GARDEÑES, M. ROMANCE, I. SENDINA-NADAL, Z. WANG, AND M. ZANIN, *The structure and dynamics of multilayer networks*, Physics Reports, 544 (2014), pp. 1–122.
- [10] P. BONACICH, *Factoring and weighting approaches to clique identification*, Journal of Mathematical Sociology, 2 (1972), pp. 113–120.
- [11] S. BRIN AND L. PAGE, *Anatomy of a large-scale hypertextual web search engine*, Proceedings of the Seventh International World Wide Web Conference, (1998), pp. 107–117.
- [12] T. CALLAGHAN, M. A. PORTER, AND P. J. MUCHA, *Random walker ranking for NCAA Division I-A football*, American Mathematical Monthly, 114 (2007), pp. 761–777.
- [13] A. CARDILLO, J. GÓMEZ-GARDENES, M. ZANIN, M. ROMANCE, D. PAPO, F. DEL POZO, AND S. BOCCALETTI, *Emergence of network features from multiplexity*, Scientific Reports, 3 (2013), p. 1344.
- [14] T. CHAKRABORTY AND R. NARAYANAM, *Cross-layer betweenness centrality in multiplex networks with applications*, in Data Engineering (ICDE), 2016 IEEE 32nd International Conference on, IEEE, 2016, pp. 397–408.
- [15] T. P. CHARTIER, E. KREUTZER, A. N. LANGVILLE, AND K. E. PEDINGS, *Sensitivity and stability of ranking vectors*, SIAM Journal on Scientific Computing, 33 (2011), pp. 1077–1102.
- [16] I. CHEN, M. BENZI, H. H. CHANG, AND V. S. HERTZBERG, *Dynamic communicability and epidemic spread: A case study on an empirical dynamic contact network*, Journal of Complex Networks, 5 (2016), pp. 274–302.
- [17] M. COSCIA, G. ROSSETTI, D. PENNACCHIOLI, D. CECCARELLI, AND F. GIANNOTTI, *You know because i know: A multidimensional network approach to human resources problem*, in Proceedings of the 2013 IEEE/ACM International Conference on Advances in Social Networks Analysis and Mining, ACM, 2013, pp. 434–441.
- [18] E. COZZO, G. FERRAZ DE ARRUDA, F. A. RODRIGUES, AND Y. MORENO, *Multiplex Networks: Basic Formalism and Structural Properties*, Springer-Verlag, 2018.
- [19] C. DE BACCO, D. B. LARREMORE, AND C. MOORE, *A physical model for efficient ranking in networks*, Science advances, 4 (2018), p. eaar8260.
- [20] M. DE DOMENICO, S. SASAI, AND A. ARENAS, *Mapping multiplex hubs in human functional brain networks*, Frontiers in Neuroscience, 10 (2016), p. 326.
- [21] M. DE DOMENICO, A. SOLÉ-RIBALTA, E. COZZO, M. KIVELÄ, Y. MORENO, M. A. PORTER, S. GÓMEZ, AND A. ARENAS, *Mathematical formulation of multilayer networks*, Physical Review X, 3 (2013), p. 041022.
- [22] M. DE DOMENICO, A. SOLÉ-RIBALTA, E. OMODEI, S. GÓMEZ, AND A. ARENAS, *Ranking in interconnected multilayer networks reveals versatile nodes*, Nature Communications, 6 (2015), p. 6868.
- [23] M. DE DOMENICO, A. SOLÉ-RIBALTA, E. OMODEI, S. GÓMEZ, AND A. ARENAS, *Ranking in interconnected multilayer networks reveals versatile nodes*, Nature Communications, 6 (2015), p. 6868.
- [24] D. R. DEFORD, *Multiplex dynamics on the World Trade Web*, in International Workshop on Complex Networks and their Applications, Springer, 2017, pp. 1111–1123.
- [25] D. R. DEFORD AND S. D. PAULS, *A new framework for dynamical models on multiplex networks*, Journal of Complex Networks, 6 (2017), pp. 353–381.
- [26] C. DING AND K. LI, *Centrality ranking in multiplex networks using topologically biased random walks*, Neurocomputing, 312 (2018), pp. 263–275.
- [27] E. ESTRADA, *Communicability in temporal networks*, Physical Review E, 88 (2013), p. 042811.
- [28] M. G. EVERETT AND S. P. BORGATTI, *Networks containing negative ties*, Social Networks, 38 (2014), pp. 111–120.
- [29] C. FENU AND D. J. HIGHAM, *Block matrix formulations for evolving networks*, SIAM Journal of Matrix Analysis and Applications, 38 (2017), pp. 343–360.
- [30] J. FLORES AND M. ROMANCE, *On eigenvector-like centralities for temporal networks: Discrete vs. continuous time scales*, Journal of Computational and Applied Mathematics, 330 (2018), pp. 1041–1051.
- [31] S. FORTUNATO, C. T. BERGSTROM, K. BÖRNER, J. A. EVANS, D. HELBING, S. MILOJEVIĆ, A. M. PETERSEN, F. RADICCHI, R. SINATRA, B. UZZI, A. VESPIGNANI, L. WALTMAN, D. WANG, AND

- A.-L. BARABÁSI, *Science of science*, Science, 359 (2018).
- [32] J. H. FOWLER, T. R. JOHNSON, J. F. SPRIGGS II, S. JEON, AND P. J. WAHLBECK, *Network analysis and the law: Measuring the legal importance of precedents at the US Supreme Court*, Political Analysis, 15 (2007), pp. 324–346.
- [33] D. F. GLEICH, *PageRank beyond the Web*, SIAM Review, 57 (2015), pp. 321–363.
- [34] G. H. GOLUB AND C. F. VAN LOAN, *Matrix Computations*, Johns Hopkins University Press, third ed., 2012.
- [35] S. GÓMEZ, A. DÍAZ-GUILERA, J. GÓMEZ-GARDEÑES, C. J. PÉREZ-VICENTE, Y. MORENO, AND A. ARENAS, *Diffusion dynamics on multiplex networks*, Physical Review Letters, 110 (2013), p. 028701.
- [36] P. GONÇALVES, *Behavior modes, pathways and overall trajectories: Eigenvector and eigenvalue analysis of dynamic systems*, System Dynamics Review: The Journal of the System Dynamics Society, 25 (2009), pp. 35–62.
- [37] P. GRINDROD AND D. J. HIGHAM, *A matrix iteration for dynamic network summaries*, SIAM Review, 55 (2013), pp. 118–128.
- [38] ———, *A dynamical systems view of network centrality*, Proceedings of the Royal Society A, 470 (2014), p. 20130835.
- [39] P. GRINDROD, M. C. PARSONS, D. J. HIGHAM, AND E. ESTRADA, *Communicability across evolving networks*, Physical Review E, 83 (2011), p. 046120.
- [40] R. GUIMERÀ, S. MOSSA, A. TURTSCHI, AND L. A. N. AMARAL, *The worldwide air transportation network: Anomalous centrality, community structure, and cities' global roles*, Proceedings of the National Academy of Sciences of the USA, 102 (2005), pp. 7794–7799.
- [41] Y. Y. HAIMES AND P. JIANG, *Leontief-based model of risk in complex interconnected infrastructures*, Journal of Infrastructure systems, 7 (2001), pp. 1–12.
- [42] A. HALU, R. J. MONDRAGÓN, P. PANZARASA, AND G. BIANCONI, *Multiplex pagerank*, PLoS ONE, 8 (2013), p. e78293.
- [43] P. HOLME, *Congestion and centrality in traffic flow on complex networks*, Advances in Complex Systems, 6 (2003), pp. 163–176.
- [44] ———, *Modern temporal network theory: A colloquium*, European Physical Journal B, 88 (2015), p. 234.
- [45] P. HOLME AND J. SARAMÄKI, *Temporal networks*, Physics Reports, 519 (2012), pp. 97–125.
- [46] D.-W. HUANG AND Z.-G. YU, *Dynamic-sensitive centrality of nodes in temporal networks*, Scientific Reports, 7 (2017), p. 41454.
- [47] Q. HUANG, C. ZHAO, X. ZHANG, X. WANG, AND D. YI, *Centrality measures in temporal networks with time series analysis*, EPL (Europhysics Letters), 118 (2017), p. 36001.
- [48] J. IACOVACCI, C. RAHMEDE, A. ARENAS, AND G. BIANCONI, *Functional multiplex pagerank*, EPL (Europhysics Letters), 116 (2016), p. 28004.
- [49] H. JEONG, S. P. MASON, A.-L. BARABÁSI, AND Z. N. OLTVAI, *Lethality and centrality in protein networks*, Nature, 411 (2001), pp. 41–42.
- [50] C. E. KAMPMANN, *Feedback loop gains and system behavior*, in Proceedings of the 1996 International System Dynamics Conference, System Dynamics Society Cambridge, MA, 1996, pp. 21–25.
- [51] C. E. KAMPMANN AND R. OLIVA, *Loop eigenvalue elasticity analysis: three case studies*, System Dynamics Review: The Journal of the System Dynamics Society, 22 (2006), pp. 141–162.
- [52] D. KEMPE, J. KLEINBERG, AND É. TARDOS, *Maximizing the spread of influence through a social network*, in Proceedings of the ninth ACM SIGKDD international conference on Knowledge discovery and data mining, ACM, 2003, pp. 137–146.
- [53] H. KIM, J. TANG, R. ANDERSON, AND C. MASCOLO, *Centrality prediction in dynamic human contact networks*, Computer Networks, 56 (2012), pp. 983–996.
- [54] M. KIVELÄ, A. ARENAS, M. BARTHELEMY, J. P. GLEESON, Y. MORENO, AND M. A. PORTER, *Multilayer networks*, Journal of Complex Networks, 2 (2014), pp. 203–271.
- [55] M. KIVELÄ AND M. A. PORTER, *Isomorphisms in multilayer networks*, Transactions on Network Science and Engineering, 5 (2018), pp. 198–211.
- [56] J. KLEINBERG, *Authoritative sources in a hyperlinked environment*, Journal of the ACM (JACM), 46 (1999), pp. 604–632.
- [57] T. KOLDA AND B. BADER, *The TOPHITS model for higher-order Web link analysis*, in Workshop on Link Analysis, Counterterrorism and Security, vol. 7, 2006, pp. 26–29.

- [58] D. KRACKHARDT, *Cognitive social structures*, Social networks, 9 (1987), pp. 109–134.
- [59] R. LAMBIOTTE AND M. ROSVALL, *Ranking and clustering of nodes in networks with smart teleportation*, Physical Review E, 85 (2012), p. 056107.
- [60] A. N. LANGVILLE AND C. D. MEYER, *Google's PageRank and Beyond: The Science of Search Engine Rankings*, Princeton University Press, 2006.
- [61] E. A. LEICHT, G. CLARKSON, K. SHEDDEN, AND M. E. J. NEWMAN, *Large-scale structure of time evolving citation networks*, The European Physical Journal B, 59 (2007), pp. 75–83.
- [62] K. LERMAN, R. GHOSH, AND J. H. KANG, *Centrality metric for dynamic networks*, in Proceedings of the Eighth Workshop on Mining and Learning with Graphs, ACM, 2010, pp. 70–77.
- [63] H. LIAO, M. S. MARIANI, M. MEDO, Y.-C. ZHANG, AND M.-Y. ZHOU, *Ranking in evolving complex networks*, Physics Reports, 689 (2017), pp. 1–54.
- [64] N. LOTFI, A. H. DAROONEH, AND F. A. RODRIGUES, *Centrality in earthquake multiplex networks*, Chaos, 28 (2018), p. 063113.
- [65] M. MAGNANI, B. MICENKOVA, AND L. ROSSI, *Combinatorial analysis of multiple networks*, arXiv preprint arXiv:1303.4986, (2013).
- [66] M. MAGNANI AND L. ROSSI, *The ml-model for multi-layer social networks*, in Advances in Social Networks Analysis and Mining (ASONAM), 2011 International Conference on, IEEE, 2011, pp. 5–12.
- [67] A. V. MANTZARIS, D. S. BASSETT, N. F. WYMBS, E. ESTRADA, M. A. PORTER, P. J. MUCHA, S. T. GRAFTON, AND D. J. HIGHAM, *Dynamic network centrality summarizes learning in the human brain*, Journal of Complex Networks, 1 (2013), pp. 83–92.
- [68] A. V. MANTZARIS AND D. J. HIGHAM, *Dynamic communicability predicts infectiousness*, in Temporal Networks, Springer, 2013, pp. 283–294.
- [69] T. MARTIN, X. ZHANG, AND M. E. J. NEWMAN, *Localization and centrality in networks*, Physical Review E, 90 (2014), p. 052808.
- [70] N. MASUDA, M. A. PORTER, AND R. LAMBIOTTE, *Random walks and diffusion on networks*, Physics Reports, 716–717 (2017), pp. 1–58.
- [71] S. MOTEGI AND N. MASUDA, *A network-based dynamical ranking system for competitive sports*, Scientific Reports, 2 (2012).
- [72] P. J. MUCHA, T. RICHARDSON, K. MACON, M. A. PORTER, AND J.-P. ONNELA, *Community structure in time-dependent, multiscale, and multiplex networks*, Science, 328 (2010), pp. 876–878.
- [73] E. NATHAN, J. FAIRBANKS, AND D. BADER, *Ranking in dynamic graphs using exponential centrality*, in International Workshop on Complex Networks and their Applications, Springer, 2017, pp. 378–389.
- [74] H. NAYAR, B. A. MILLER, K. GEYER, R. S. CACERES, S. T. SMITH, AND R. R. NADAKUDITI, *Improved hidden clique detection by optimal linear fusion of multiple adjacency matrices*, in Signals, Systems and Computers, 2015 49th Asilomar Conference on, IEEE, 2015, pp. 1520–1524.
- [75] M. E. J. NEWMAN, *Networks*, Oxford University Press, second ed., 2018.
- [76] M. K.-P. NG, X. LI, AND Y. YE, *Multirank: Co-ranking for objects and relations in multi-relational data*, in Proceedings of the 17th ACM SIGKDD international conference on Knowledge discovery and data mining, ACM, 2011, pp. 1217–1225.
- [77] N. OTTER, M. A. PORTER, U. TILLMANN, P. GRINDROD, AND H. A. HARRINGTON, *A roadmap for the computation of persistent homology*, European Physical Journal — Data Science, 6 (2017), pp. 1–38.
- [78] L. PAGE, S. BRIN, R. MOTWANI, AND T. WINOGRAD, *The PageRank citation ranking: Bringing order to the Web*, Technical Report 1999-66, Stanford InfoLab, November 1999. Available at <http://ilpubs.stanford.edu:8090/422/>.
- [79] A. R. PAMFIL, S. D. HOWISON, R. LAMBIOTTE, AND M. A. PORTER, *Relating modularity maximization and stochastic block models in multilayer networks*, arXiv preprint arXiv:1804.01964, (2018).
- [80] R. PAN AND J. SARAMÄKI, *Path lengths, correlations, and centrality in temporal networks*, Physical Review E, 84 (2011), p. 016105.
- [81] R. PASTOR-SATORRAS AND C. CASTELLANO, *Eigenvector localization in real networks and its implications for epidemic spreading*, Journal of Statistical Physics, 173 (2018), pp. 1110–1123.
- [82] M. A. PORTER, *WHAT IS... A multilayer network*, Notices of the American Mathematical Society, 65 (2018), pp. 1419–1423.
- [83] M. PÓSFAL, N. BRAUN, B. A. BEISNER, B. MCCOWAN, AND R. M. D'SOUZA, *Consensus ranking for multi-objective interventions in multiplex networks*, arXiv preprint arXiv:1903.02059, (2019).

- [84] S. PRAPROTNIK AND V. BATAGELJ, *Spectral centrality measures in temporal networks*, *Ars Mathematica Contemporanea*, 11 (2015), pp. 11–33.
- [85] MATHEMATICS GENEALOGY PROJECT, *The Mathematics Genealogy Project*, 2009. <http://www.genealogy.ams.org>, data provided 19 October 2009.
- [86] F. RADICCHI AND A. ARENAS, *Abrupt transition in the structural formation of interconnected networks*, *Nature Physics*, 9 (2013), pp. 717–720.
- [87] C. RAHMEDE, J. IACOVACCI, A. ARENAS, AND G. BIANCONI, *Centralities of nodes and influences of layers in large multiplex networks*, *Journal of Complex Networks*, (2017).
- [88] A. REIFFERS-MASSON AND V. LABATUT, *Opinion-based centrality in multiplex networks: A convex optimization approach*, *Network Science*, 5 (2017), pp. 213–234.
- [89] J. G. RESTREPO, E. OTT, AND B. R. HUNT, *Characterizing the dynamical importance of network nodes and links*, *Physical Review Letters*, 97 (2006), p. 094102.
- [90] L. E. C. ROCHA AND N. MASUDA, *Random walk centrality for temporal networks*, *New Journal of Physics*, 16 (2014), p. 063023.
- [91] M. ROMANCE, L. SOLÁ, J. FLORES, E. GARCÍA, A. G. DEL AMO, AND R. CRIADO, *A Perron–Frobenius theory for block matrices associated to a multiplex network*, *Chaos, Solitons & Fractals*, 72 (2015), pp. 77–89.
- [92] R. A. ROSSI AND D. F. GLEICH, *Dynamic PageRank using evolving teleportation*, in *Algorithms and Models for the Web Graph*, Springer, 2012, pp. 126–137.
- [93] S. SAAVEDRA, S. POWERS, T. MCCOTTER, M. A. PORTER, AND P. J. MUCHA, *Mutually-antagonistic interactions in baseball networks*, *Physica A*, 389 (2010), pp. 1131–1141.
- [94] L. SOLÁ, M. ROMANCE, R. CRIADO, J. FLORES, A. G. DEL AMO, AND S. BOCCALETTI, *Eigenvector centrality of nodes in multiplex networks*, *Chaos*, 23 (2013), p. 033131.
- [95] A. SOLÉ-RIBALTA, M. DE DOMENICO, S. GÓMEZ, AND A. ARENAS, *Centrality rankings in multiplex networks*, in *Proceedings of the 2014 ACM Conference on Web Science*, ACM, 2014, pp. 149–155.
- [96] ———, *Random walk centrality in interconnected multilayer networks*, *Physica D*, 323 (2016), pp. 73–79.
- [97] A. SOLÉ-RIBALTA, M. DE DOMENICO, N. E. KOUVARIS, A. DIAZ-GUILERA, S. GOMEZ, AND A. ARENAS, *Spectral properties of the Laplacian of multiplex networks*, *Physical Review E*, 88 (2013), p. 032807.
- [98] C. SPATOCCHIO, G. STILO, AND C. DOMENICONI, *A new framework for centrality measures in multiplex networks*, arXiv preprint arXiv:1801.08026, (2018).
- [99] T. TAKAGUCHI, Y. YANO, AND Y. YOSHIDA, *Coverage centralities for temporal networks*, *The European Physical Journal B*, 89 (2016), pp. 1–11.
- [100] J. TANG, M. MUSOLESI, C. MASCOLO, V. LATORA, AND V. NICOSIA, *Analysing information flows and key mediators through temporal centrality metrics*, in *Proc. of the 3rd Workshop on Social Network Systems - SNS '10*, 2010, pp. 1–6.
- [101] S. TAVASSOLI AND K. A. ZWEIG, *Most central or least central? how much modeling decisions influence a node's centrality ranking in multiplex networks*, arXiv preprint arXiv:1606.05468, (2016).
- [102] D. TAYLOR, *Code release: Supracentrality*; available at <https://github.com/taylordr/Supracentrality>.
- [103] ———, *Data release: Ph.D. exchange in the Mathematical Genealogy Project*; available at <https://sites.google.com/site/danetaylorresearch/data>.
- [104] D. TAYLOR AND D. B. LARREMORE, *Social climber attachment in forming networks produces a phase transition in a measure of connectivity*, *Physical Review E*, 86 (2012), p. 031140.
- [105] D. TAYLOR, S. A. MYERS, A. CLAUSET, M. A. PORTER, AND P. J. MUCHA, *Eigenvector-based centrality measures for temporal networks*, *Multiscale Modeling & Simulation*, 15 (2017), pp. 537–574.
- [106] D. TAYLOR AND J. G. RESTREPO, *Network connectivity during mergers and growth: Optimizing the addition of a module*, *Physical Review E*, 83 (2011), p. 066112.
- [107] ———, *A network-specific approach to percolation in complex networks with bidirectional links*, *EPL (Europhysics Letters)*, 98 (2012), p. 16007.
- [108] D. TAYLOR, P. S. SKARDAL, AND J. SUN, *Synchronization of heterogeneous oscillators under network modifications: Perturbation and optimization of the synchrony alignment function*, *SIAM Journal on Applied Mathematics*, 76 (2016), pp. 1984–2008.
- [109] H. TONG, B. A. PRAKASH, T. ELIASSI-RAD, M. FALOUTSOS, AND C. FALOUTSOS, *Gelling, and melting, large graphs by edge manipulation*, in *Proceedings of the 21st ACM international conference on Information and knowledge management*, ACM, 2012, pp. 245–254.

-
- [110] F. TUDISCO, F. ARRIGO, AND A. GAUTIER, *Node and layer eigenvector centralities for multiplex networks*, SIAM Journal on Applied Mathematics, 78 (2018), pp. 853–876.
 - [111] M. VAIANA AND S. F. MULDOON, *Multilayer brain networks*, Journal of Nonlinear Science, (2018). Available at <https://doi.org/10.1007/s00332-017-9436-8>.
 - [112] E. VALDANO, L. FERRERI, C. POLETTO, AND V. COLIZZA, *Analytical computation of the epidemic threshold on temporal networks*, Physical Review X, 5 (2015), p. 021005.
 - [113] W. H. WEIR, S. EMMONS, R. GIBSON, D. TAYLOR, AND P. J. MUCHA, *Post-processing partitions to identify domains of modularity optimization*, Algorithms, 10 (2017), p. 93.
 - [114] M. J. WILLIAMS AND M. MUSOLESI, *Spatio-temporal networks: Reachability, centrality and robustness*, Royal Society Open Science, 3 (2016).
 - [115] K. YOU, R. TEMPO, AND L. QIU, *Distributed algorithms for computation of centrality measures in complex networks*, IEEE Transactions on Automatic Control, 62 (2017), pp. 2080–2094.
 - [116] M. YU, M. ENGELS, A. HILLEBRAND, E. CW VAN STRAATEN, A. A. GOUW, C. TEUNISSEN, W. M. VAN DER FLIER, P. SCHELTENS, AND C. J. STAM, *Selective impairment of hippocampus and posterior hub areas in Alzheimer’s disease: An MEG-based multiplex network study*, Brain, 140 (2017), pp. 1466–1485.

SUPPLEMENTARY MATERIALS: Tunable Eigenvector-Based Centralities for Multiplex and Temporal Networks *

Dane Taylor[†], Mason A. Porter[‡], and Peter J. Mucha[§]

Here, we provide more information for our study of the pedagogical network (Sec. SM1), multiplex airline network (Sec. SM2), and Ph.D. exchange network (Sec. SM3).

SM1. Extended Study of our Pedagogical Example. In this section, we present an extended study of our numerical experiment (see Sec. 3.3 of the main text) in which we examine the multiplex network in Fig. 1(a) of the main text. Recall for this network that the interlayer coupling between layers 3 and 4 differs from that of the other interlayer couplings. (See the dashed lines in Fig. 1(a).) In Sec. 3.3, we set $\tilde{A}_{34} = \tilde{A}_{43} = 0.01$, whereas we set $\tilde{A}_{tt'} = 1$ for the other interlayer couplings.

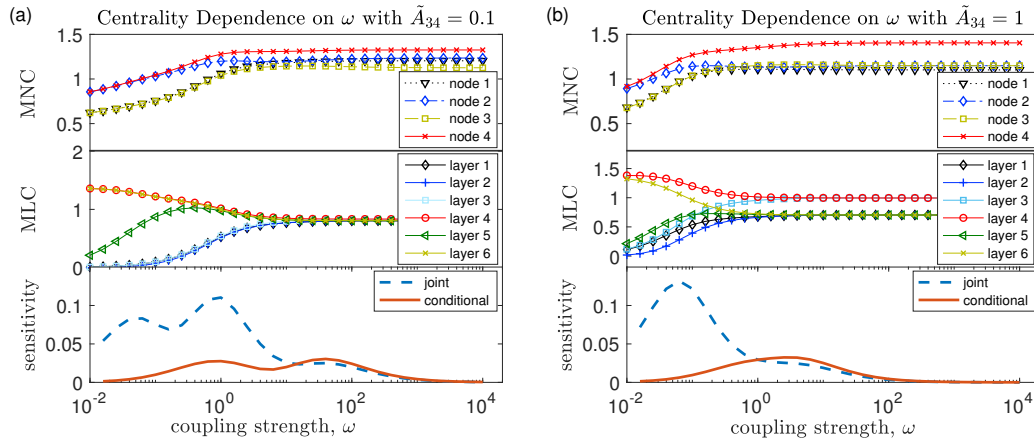


Figure SM1. Eigenvector supracentrality results for our pedagogical multiplex network in which the coupling between layers 3 and 4 differs from the coupling between the other layers. In panels (a) and (b), we report the same results as in Fig. 3(b) in the main text (for which we used $\tilde{A}_{34} = \tilde{A}_{43} = 0.01$), except that now we use (a) $\tilde{A}_{34} = \tilde{A}_{43} = 0.1$ and (b) $\tilde{A}_{34} = \tilde{A}_{43} = 1$. Note in panel (b) that the curves for “sensitivity”, which we measure in terms stepwise magnitudes of change (specifically, $\|\mathbf{W}(\omega_s) - \mathbf{W}(\omega_{s-1})\|_F$ and $\|\mathbf{Z}(\omega_s) - \mathbf{Z}(\omega_{s-1})\|_F$), are no longer bimodal.

In Fig. SM1, we now explore two other choices: (a) $\tilde{A}_{34} = \tilde{A}_{43} = 0.1$ and (b) $\tilde{A}_{34} = \tilde{A}_{43} = 1$. We plot the marginal node centralities (MNCs), marginal layer centralities (MLCs), and “sensitivity” of the joint and conditional centralities across a range of coupling strengths ω . Our measures of sensitivity are the stepwise magnitudes of change (i.e., $\|\mathbf{W}(\omega_s) - \mathbf{W}(\omega_{s-1})\|_F$

*

[†]Department of Mathematics, University at Buffalo, State University of New York, Buffalo, NY 14260, USA

[‡]Department of Mathematics, University of California, Los Angeles, CA 90095, USA

[§]Carolina Center for Interdisciplinary Applied Mathematics, Department of Mathematics and Department of Applied Physical Sciences, University of North Carolina, Chapel Hill, NC 27599, USA

SM1

and $\|\mathbf{Z}(\omega_s) - \mathbf{Z}(\omega_{s-1})\|_F$. In panel (b), note that the curves are no longer bimodal, implying that a stable intermediate regime vanishes as we increase \tilde{A}_{34} . Intuitively, this occurs because the network associated with the interlayer-adjacency matrix $\tilde{\mathbf{A}}$ of Fig. 1(a) no longer has two well-separated communities if $\tilde{A}_{34} = \tilde{A}_{43} = 1$.

SM2. Extended Study of European Airport Rankings. In this section, we discuss additional results for our study of a European airline transportation multiplex network (with data from [SM1]) from Sec. 5.1 of the main text. Recall that the network has $N = 417$ European airports, which we identify to be in the largest strongly connected component of an aggregation (which we obtained from summing the layers' adjacency matrices) of the multiplex network. There are $T = 37$ layers, each of which encodes the flight patterns between airports for a single airline company. In Table SM1, we list these airline companies. For each layer, we indicate the number $M_t = \frac{1}{2} \sum_{ij} A_{ij}^{(t)}$ of intralayer edges and the spectral radius $\lambda_1^{(t)}$ of the layer's associated adjacency matrix $\mathbf{A}^{(t)}$. The layer that represents Ryanair ($t = 2$) has the most edges (with almost twice as many as any other airline) and the largest spectral radius. We provide an illustration of the multiplex network in Fig. SM2.

In Sec. 5.1 of main text, we studied supracentralities for the European airline transportation multiplex network using the layers' adjacency matrices as their centrality matrices $\mathbf{C}^{(t)} = \mathbf{A}^{(t)}$ (so these are eigenvector supracentralities); and we found that the Ryanair network dominates the supracentralities in the weak-coupling limit due to eigenvector localization.

Table SM1

List of European airline companies, which we represent as layers in a multiplex network. For each layer, we report the number M_t of undirected edges and the spectral radius $\lambda_1^{(t)}$ of its associated adjacency matrix $\mathbf{A}^{(t)}$. The ordering has been chosen to correspond to [SM1].

Layer (t)	Airline Name	M_t	$\lambda_1^{(t)}$	Layer t	Airline Name	M_t	$\lambda_1^{(t)}$
1	Lufthansa	244	14.5	20	LOT Polish Air.	55	6.8
2	Ryanair	601	19.3	21	Vueling Airlines	63	6.8
3	easyJet	307	14.0	22	Air Nostrum	69	6.4
4	British Airways	66	6.6	23	Air Lingus	108	6.7
5	Turkish Airlines	118	9.9	24	Germanwings	67	7.4
6	Air Berlin	184	11.3	25	Pegasus Airlines	58	6.7
7	Air France	69	7.2	26	NetJets	180	8.2
8	Scandinavian Air.	110	8.9	27	Transavia Holland	57	6.0
9	KLM	62	7.9	28	Niki	37	4.7
10	Alitalia	93	8.8	29	SunExpress	67	7.8
11	Swiss Int. Air Lines	60	7.3	30	Aegean Airlines	53	6.5
12	Iberia	35	5.8	31	Czech Airlines	41	6.4
13	Norwegian Air Shu.	67	8.1	32	European Air Trans.	73	6.8
14	Austrian Airlines	74	8.1	33	Malev Hungarian Air.	34	5.8
15	Flybe	99	8.5	34	Air Baltic	45	6.4
16	Wizz Air	92	6.5	35	Wideroe	40	5.6
17	TAP Portugal	53	7.0	36	TNT Airways	61	6.2
18	Brussels Airlines	43	6.6	37	Olympic Air	43	6.2
19	Finnair	42	6.4				

SM2

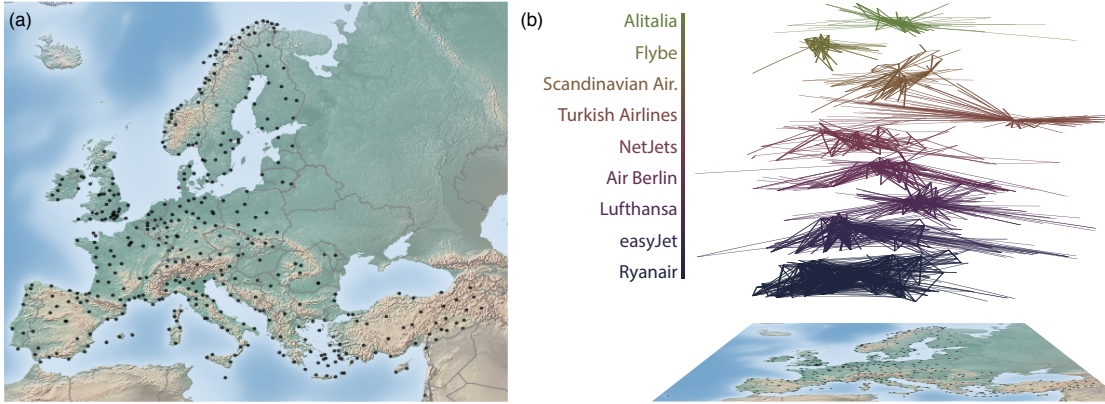


Figure SM2. Multilayer network encoding flights between European airports. (a) Map of airport locations. (b) Illustration of the nine network layers (i.e., airlines) that have the most edges.

Specifically, as we illustrated in Fig. 4(a) of the main text, $\mathfrak{v}(\omega)$ localizes onto layer $t = 2$. Corollary 4.3 of the main text describes this phenomenon, which occurs because the centrality matrix for Ryanair has the largest spectral radius.

We now study supracentralities when the layers' centrality matrices are PageRank matrices. (See Definition 2.5 in the main text.) In Table SM2, we list the airports with the largest MLCs for small, intermediate, and large values of the coupling strength ω . Unsurprisingly, there is some overlap with the top-ranked airports in Table 2 of the main text (which is based on eigenvector supracentralities). For example, LEMD (Adolfo Suárez Madrid–Barajas Airport) makes the top-10 list for all values of ω in both tables. However, most of the top-ranked airports are different. In particular, for $\omega \geq 0.1$, the top-ranked airports are LTBA, EBLG,

Table SM2

European airports with the top marginal node centralities (MNCs) for coupling strengths $\omega \in \{0.01, 1, 100\}$, which correspond to the regimes of weak, intermediate, and strong coupling. We show results for when the layers' centrality matrices are PageRank matrices and the interlayer-adjacency matrix is $\tilde{\mathbf{A}} = \mathbf{1}\mathbf{1}^T$. We indicate airports using their International Civil Aviation Organization (ICAO) codes.

Rank	$\omega = 10^{-4}$		$\omega = 10^{-1}$		$\omega = 10^2$	
	Airport	MNC	Airport	MNC	Airport	MNC
1	EHAM	0.406	LTBA	0.802	LTBA	0.929
2	LOWW	0.373	EBLG	0.732	EBLG	0.866
3	LTBA	0.372	LTFJ	0.700	EVRA	0.818
4	EGKK	0.365	EVRA	0.695	LTFJ	0.791
5	LEMD	0.363	EHAM	0.662	EHAM	0.725
6	LTFJ	0.344	EGKK	0.653	LOWW	0.699
7	LFPG	0.337	LOWW	0.633	EGKK	0.698
8	LGAV	0.333	EIDW	0.586	EIDW	0.656
9	EGLL	0.328	EGSS	0.583	EGSS	0.631
10	EIDW	0.328	LEMD	0.554	LEMD	0.596

SM3

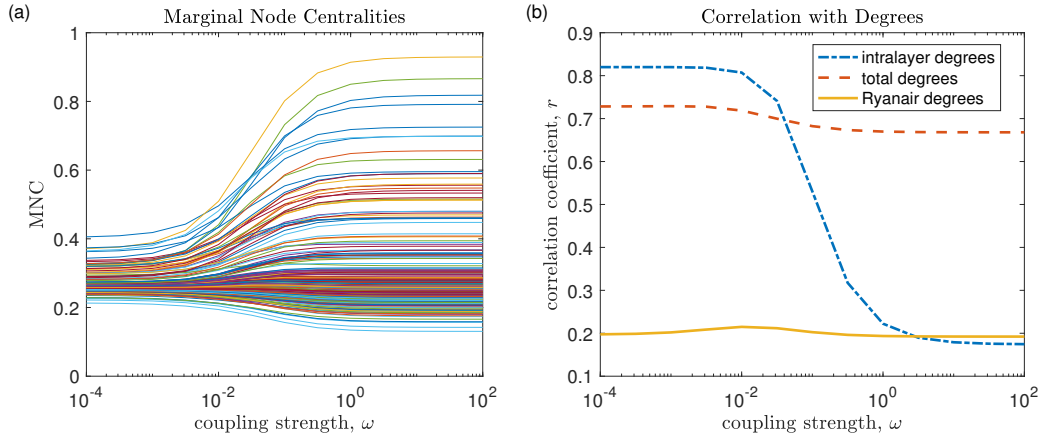


Figure SM3. Supracentralities for the multiplex European airline network with the layers' centrality matrices given by their PageRank matrices. (a) Airport MNCs versus intralayer coupling strength ω . (b) Pearson correlation coefficients for comparing PageRank supracentralities and node degrees.

LTFJ, and EVRA for PageRank supracentrality; and none of these airports are in Table 2 of the main text. This is unsurprising, as it is well-known for monolayer networks that although PageRank and eigenvector centrality are correlated with each other, they identify different types of node importances.

We can gain insight into one of the main causes for these differences by examining the limit of small ω . In Fig. 5(b) of the main text, we observed that the marginal centralities correlated very strongly with the intralayer node degrees in the Ryanair layer (but not in the other layers). However, as we can see in Fig. SM3(b), the PageRank MNCs paint a very different picture. Specifically, for small values of ω , the conditional centralities correlate strongly with the intralayer node degrees of all layers. In other words, for eigenvector supracentrality, the Ryanair layer dominates, and the supracentralities largely reflect the intralayer node degrees of this single layer. By contrast, for PageRank supracentralities, the Ryanair layer is not dominant. Whether or not there is such domination depends on if we observe eigenvector localization as $\omega \rightarrow 0^+$, as described by Thm. 4.2 and Cor. 4.3 of the main text. In this example, localization occurs for eigenvector supracentrality but not for PageRank supracentrality. There is no such localization in the latter case, because PageRank matrices are transition matrices for Markov chains, so they have a spectral radius of 1.

SM3. Extended Study of United States Mathematical-Sciences Doctoral Program Rankings. In this section, we present additional results for our study (see Sec. 5.2 of the main text) of supracentralities in a temporal network of the graduation and hiring of mathematical-science Ph.D. recipients between U.S. universities. (The data set, released with [SM4] and available at [SM3], was compiled from the Mathematics Genealogy Project [SM2].) In Table SM3, we list the universities with the top MNCs for when the layers' centrality matrices are given by their authority matrices. (See Definition 2.4 in the main text.) The interlayer-adjacency matrix $\tilde{\mathbf{A}}$ is given by Eq. (5.5) of the main text. We show results for several choices of the layer teleportation parameter γ and interlayer coupling strength ω . Observe that the

Table SM3

Top MNCs (see Definition 3.3 of the main text) for U.S. mathematical-science programs when the layers' centrality matrices are authority matrices and the interlayer-adjacency matrix given by Eq. (5.5) of the main text. We show results for three choices of the layer teleportation parameter γ and interlayer coupling strength ω .

Rank	MNC, $(\gamma, \omega) = (10^{-2}, 1)$		MNC, $(\gamma, \omega) = (10^{-2}, 10^2)$		MNC, $(\gamma, \omega) = (10^{-3}, 10^2)$	
	University	\hat{x}_i	University	\hat{x}_i	University	\hat{x}_i
1	MIT	0.91	MIT	5.28	MIT	3.47
2	U Washington	0.23	UC Berkeley	2.28	UC Berkeley	1.72
3	Boston U	0.15	Stanford	1.84	Stanford	1.28
4	U Michigan	0.12	Princeton	1.42	Harvard	0.97
5	Brown	0.12	Harvard	1.28	Princeton	0.96
6	UCLA	0.111	Cornell	1.23	Cornell	0.89
7	Carnegie Mellon	0.11	UIUC	1.18	UIUC	0.77
8	Purdue	0.11	Washington	1.13	UCLA	0.75
9	USC	0.11	U Michigan	1.12	Wisconsin-Madison	0.74
10	U of Georgia	0.11	UCLA	1.09	U Michigan	0.66

particular ordering of the top-ranked schools depends sensitively on the choices for γ and ω . However, we typically obtain the same set of universities near the top. MIT, for example, is almost always ranked first in the entire (γ, ω) parameter space.

In Fig. SM4, we illustrate the effect of ω on the authority supracentralities for a layer teleportation parameter value of $\gamma = 10^{-2}$. In panels (a) and (b), we show the layers' MLCs and nodes' MNCs, respectively. We observe three qualitative regimes: weak, intermediate, and strong coupling. The insets in (a) and (b) compare observed conditional node centralities for $\omega = 1$ and $\omega = 10^4$, respectively, to the asymptotic values from Thms. 4.2 and 4.7,



Figure SM4. Supracentralities of the Ph.D. exchange network with the layers' centrality matrices given by their authority matrices and the interlayer-adjacency matrix given by Eq. (5.5) of the main text with layer teleportation parameter $\gamma = 10^{-2}$. (a) MLCs versus ω . (b) MNCs versus ω . The insets in (a) and (b) compare observed conditional node centralities for $\omega = 1$ and $\omega = 10^4$, respectively, to the asymptotic values from Thms. 4.2 and 4.7, respectively. (c) We compute the Pearson correlation to measure the similarity between authority supracentralities and node degrees.

respectively.

In Fig. SM4(c), we plot (as a function of ω) the Pearson correlation coefficient r between node degrees and authority supracentralities for three cases: total degrees $\{\bar{d}_i\}$ and conditional node centralities, averaged across layers; intralayer degrees (i.e., $d_i^{(t)} = \sum_j A_{ij}^{(t)}$) and conditional centralities; and degrees in layer $t = 1966$ (i.e., $d_i^{(1966)} = \sum_j A_{ij}^{(1966)}$) and conditional centralities, again averaged across the layers. The gold dashed curve indicates the Pearson correlation coefficient between the MNCs and the values $\sum_j C_{ij}^{(1966)} = \sum_{k,j} A_{ki}^{(1966)} A_{kj}^{(1966)}$, which give a first-order approximation to the authority scores for the dominant layer ($t = 1966$). (See footnote 3 of the main text.) For very large values of ω , note that the authority supracentralities correlate strongly with the nodes' total degrees. For all values of ω , the supracentralities correlate strongly with the row sums of the matrices $\mathbf{A}^{(1966)}$ and $\mathbf{C}^{(1966)}$ for layer $t = 1966$ (the spectral radii of these matrices are larger than those of the matrices that are associated with the other layers); and they give the largest correlation for small ω .

REFERENCES

- [1] A. CARDILLO, J. GÓMEZ-GARDENES, M. ZANIN, M. ROMANCE, D. PAPO, F. DEL POZO, AND S. BOCCALETTI, *Emergence of network features from multiplexity*, Scientific Reports, 3 (2013), p. 1344.
- [2] MATHEMATICS GENEALOGY PROJECT, *The Mathematics Genealogy Project*, 2009. <http://www.genealogy.ams.org>, data provided 19 October 2009.
- [3] D. TAYLOR, *Data release: Ph.D. exchange in the Mathematical Genealogy Project; available at <https://sites.google.com/site/danetaylorresearch/data>*.
- [4] D. TAYLOR, S. A. MYERS, A. CLAUSET, M. A. PORTER, AND P. J. MUCHA, *Eigenvector-based centrality measures for temporal networks*, Multiscale Modeling & Simulation, 15 (2017), pp. 537–574.